Supplementary information

The electronic effect on the electrocatalytic hydrogen evolution reaction of silicon(IV) corrole complexes

Liang-Hong Liu, Feng Li, Xu-You Cao, Qing-Hua Yu, Zhen-Wu Liu, Hao Zhang, Fu-Rong Wang *, and Hai-Yang Liu *

School of Chemistry and Chemical Engineering, Guangdong Provincial Key Laboratory of Fuel Cell Technology, South China University of Technology, Guangzhou 510641, P.R. China

*Corresponding Author: chhyliu@scut.edu.cn

1. General informations

All reagents were purchased commercially and were used without further purification unless otherwise pointed out. ^{1}H and ^{19}F NMR spectra were recorded on a Bruker Avance III 500 MHz NMR spectrometer. The NMR spectra were referenced to the $CDCl_3$ residual solvent signal (7.26 ppm). UV-vis spectra in CH_2Cl_2 were recorded using a Hitachi U-3010 spectrophotometer at room temperature. High-resolution mass spectra (HRMS) were obtained using the Bruker microQ-TOF-QII high resolution spectrometer in the electrospray ionization (ESI) mode using Bruker Daltonics coupled to a Water Acquinty system. X-ray photoelectron spectroscopy (XPS) was measured using an Axis Ultra DLD spectrophotometer, correcting the binding energies by comparing to C 1s peak (284.8 eV) by the adventitious hydrocarbon. Electrochemical measurements were performed with a CHI-660E electrochemical workstation at room temperature under saturated N_2. The three-electrode cell had glass carbon (GC) as the working electrode, graphite rod as the counter electrode, saturated $Ag/AgNO_3$ as the reference electrode in DMF, and Ag/AgCl as the reference electrode in aqueous solutions. Ferrocene was added as an internal standard in DMF. Controlled potential electrolysis (CPE) test was performed in a single electrolytic cell filled with 20 mL of buffer solution (CH_3CN: H_2O 1:2) with 0.1 M KCl and 0.25 M KH_2PO_4.

2. Synthesis of corroles

5,10,15-tris (pentafluorophenyl) corrole (**$F_{15}C$**), 5,15-bis (pentafluorophenyl)-10-(phen-yl) corrole (**$F_{10}C$**), 5,15-bis (phenyl)-10-(pentafluoropheny) corrole (**F_5C**), 5,10,15-tris (phe-nyl) corrole (**F_0C**) were prepared by previously published procedures.[1-3]

5,10,15-tris (pentafluorophenyl) corrole ($F_{15}C$)

^{1}H NMR (500 MHz, Chloroform-*d*) δ 9.10 (d, *J* = 4.2 Hz, 2H), 8.78 (d, *J* = 4.6 Hz, 2H), 8.58 (dd, *J* = 21.0, 3.8 Hz, 4H). ^{19}F NMR (471 MHz, Chloroform-*d*) δ -137.45 (d, *J* = 257.0 Hz, 6F), -152.43 (d, *J* = 272.7 Hz, 3F), -161.62 (d, *J* = 219.8 Hz, 6F). HR-MS: m/z calculated for $C_{37}H_{12}F_{15}N_4^+$: 797.0817 $[M+H]^+$; found: 797.0824.

5,15-bis (pentafluorophenyl)-10-(phenyl) corrole ($F_{10}C$)

^{1}H NMR (500 MHz, Chloroform-*d*) δ 9.11 (d, *J* = 4.3 Hz, 2H), 8.71 (s, 4H), 8.57 (d, *J* = 4.3 Hz, 2H), 8.18 (d, *J* = 3.6 Hz, 2H), 7.80 – 7.74 (m, 3H). ^{19}F NMR (471 MHz, Methylene Chloride-d_2) δ -139.77 (dd, *J* = 24.3, 8.5 Hz, 4F), -154.77 (d, *J* = 20.7 Hz, 2F), -163.45 – -164.07 (m, 4F). HR-MS: m/z calculated for $C_{37}H_{17}F_{10}N_4^+$: 707.1288 $[M+H]^+$; found: 707.1293.

5,15-bis (phenyl)-10-(pentafluoropheny) corrole (F_5C)

^{1}H NMR (500 MHz, Chloroform-*d*) δ 8.91 (d, *J* = 60.5 Hz, 4H), 8.57 – 8.28 (m, 8H), 7.83 (d, *J* = 27.3 Hz, 6H). ^{19}F NMR (471 MHz, Chloroform-*d*) δ -136.85 – -138.44 (m, 2F), -153.76 (d, *J* = 128.5 Hz, 1F), -162.30 (d, *J* = 129.3 Hz, 2F). HR-MS: m/z calculated for $C_{37}H_{22}F_5N_4^+$: 617.1759 $[M+H]^+$; found: 617.1763.

5,10,15-tris (phenyl) corrole (F_0C)

^{1}H NMR (500 MHz, Chloroform-*d*) δ 8.98 – 8.81 (m, 4H), 8.65 – 8.10 (m, 10H), 7.93 – 7.64 (m, 9H). HR-MS: m/z calculated for $C_{37}H_{27}N_4^+$: 527.2230 [M+H]$^+$; found: 527.2227.

5,10,15-tris (pentafluorophenyl) silicon (IV) corrole ($F_{15}C$-Si)

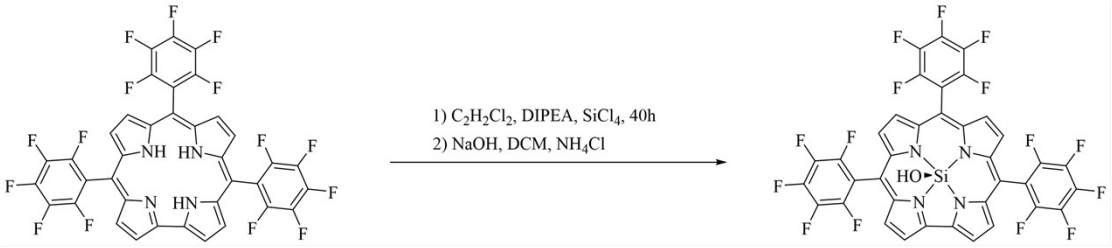

Fig. S1 Synthetic routes of Si corrole.

The synthesis method of silicon corrole complexes was thoroughly detailed in previous reports,[4] and our research has made some modifications to it. Taking the synthesis of **$F_{15}C$-Si** as an example: Free base **$F_{15}C$** (199 mg, 0.25 mmol) was dissolved in 1,2-dichloroethane (38 mL) and DIPEA (N, N-diisopropylethylamine, 6.5 mL ,38 mmol). Tetrachlorosilane (1.4 mL, 12.5 mmol) was slowly added to the obtained solution. The reaction mixture was stirred at 60 °C for 40 hours. The reaction mixture was then washed with aqueous NaOH (1 M) and extracted with dichloromethane. The organic extract was neutralized with an aqueous solution of NH_4Cl and washed with saturated saline. The organic extract was dried with anhydrous Na_2SO_4 and after removing the solvent under reduced pressure, the crude product was purified by silica gel chromatography column by using a solvent system (V_{DCM}: V_{Hex} = 4:1) as eluent. After recrystallization obtain black solid (171.1 mg, yield 81.7%). ^{1}H NMR (500 MHz, Chloroform-*d*) δ 9.54 (d, *J* = 4.4 Hz, 2H), 9.11 (d, *J* = 4.9 Hz, 2H), 9.07 (d, *J* = 4.4 Hz, 2H), 8.93 (d, *J* = 4.8 Hz, 2H). ^{19}F NMR (471 MHz, Chloroform-*d*) δ -136.30 – -136.53 (m, 3F), -137.08 – -137.26 (m, 3F), -151.74 – -152.01 (m, 3F), -161.01 – -161.46 (m, 6F). ^{29}Si NMR (119 MHz, $CDCl_3$) δ -149.4. HR-MS: m/z calculated for $C_{37}H_9F_{15}N_4NaOSi^+$: 861.0198 [M+Na]$^+$; found: 861.0204.

5,15-bis (pentafluorophenyl)-10-(phenyl) silicon (IV) corrole ($F_{10}C$-Si)

The synthetic route was similar to **$F_{15}C$-Si**, after recrystallization obtain pure silicon corrole (black solid, yield 80.3%). ^{1}H NMR (500 MHz, Chloroform-*d*) δ 9.52 (d, *J* = 4.3 Hz, 2H), 9.03 (dt, *J* = 6.0, 4.6 Hz, 6H), 8.33 – 8.28 (m, 1H), 8.09 – 8.04 (m, 1H), 7.85 – 7.74 (m, 3H). ^{19}F NMR (471 MHz, Chloroform-*d*) δ -136.44 – -136.56 (m, 2F), -137.27 – -137.39 (m, 2F), -152.43 (t, *J* = 20.9 Hz, 2F), -161.36 – -161.65 (m, 4F). ^{29}Si NMR (119 MHz, $CDCl_3$) δ -149.2. HR-MS: m/z calculated for $C_{37}H_{15}F_{10}N_4OSi^+$: 749.0850 [M+H]$^+$; found: 749.0857.

5,15-bis (phenyl)-10-(pentafluoropheny) silicon (IV) corrole (F_5C-Si)

The synthetic route was similar to **F_{15}C-Si**, after recrystallization obtain pure silicon corrole (black solid, yield 77.6%). ^{1}H NMR (500 MHz, Chloroform-*d*) δ 9.28 (d, *J* = 3.4 Hz, 2H), 9.16 (d, *J* = 3.9 Hz, 2H), 8.99 (d, *J* = 3.4 Hz, 2H), 8.65 (d, *J* = 3.9 Hz, 2H), 8.30 – 8.05 (m, 4H), 7.70 (t, *J* = 7.2 Hz, 6H). ^{19}F NMR (471 MHz, Chloroform-*d*) δ -136.68 (dd, *J* = 24.4, 8.5 Hz, 1F), -137.51 (dd, *J* = 24.1, 8.6 Hz, 1F), -153.02 (t, 1F), -161.83 (dtd, *J* = 88.1, 22.6, 21.7, 8.4 Hz, 2F). ^{29}Si NMR (119 MHz, $CDCl_3$) δ -148.7. HR-MS: m/z calculated for $C_{37}H_{20}F_5N_4OSi^+$: 659.1321 $[M+H]^+$; found: 659.1321.

5,10,15-tris (phenyl) silicon (IV) corrole (F_0C-Si)

The synthetic route was similar to **F_{15}C-Si**, after recrystallization obtain pure silicon corrole (black solid, yield 71.5%). ^{1}H NMR (500 MHz, Chloroform-*d*) δ 9.37 (d, *J* = 4.3 Hz, 2H), 9.21 (d, *J* = 4.8 Hz, 2H), 9.08 (d, *J* = 4.2 Hz, 2H), 8.91 (d, *J* = 4.8 Hz, 2H), 8.41 – 8.17 (m, 4H), 8.05 (d, *J* = 6.9 Hz, 1H), 7.86 – 7.70 (m, 10H). ^{29}Si NMR (119 MHz, $CDCl_3$) δ -148.7. HR-MS: m/z calculated for $C_{37}H_{24}N_4NaOSi^+$: 591.1612 $[M+Na]^+$; found: 591.1616.

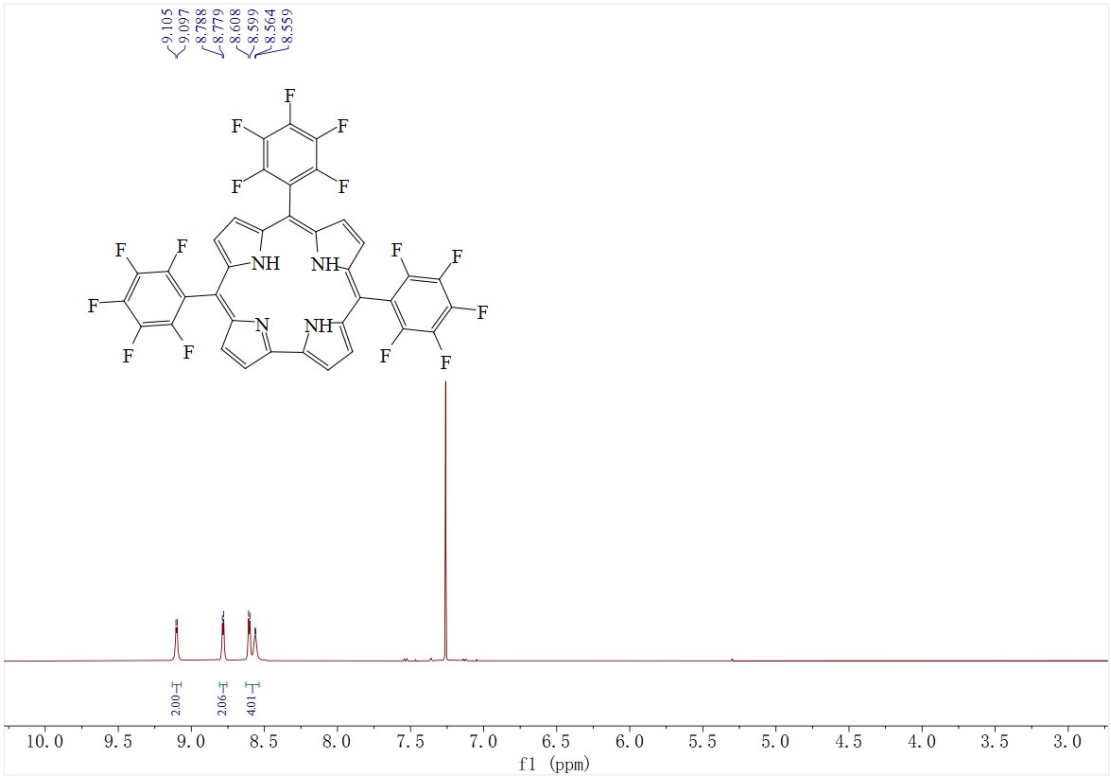

Fig. S2 ^{1}H NMR spectrum of $F_{15}C$.

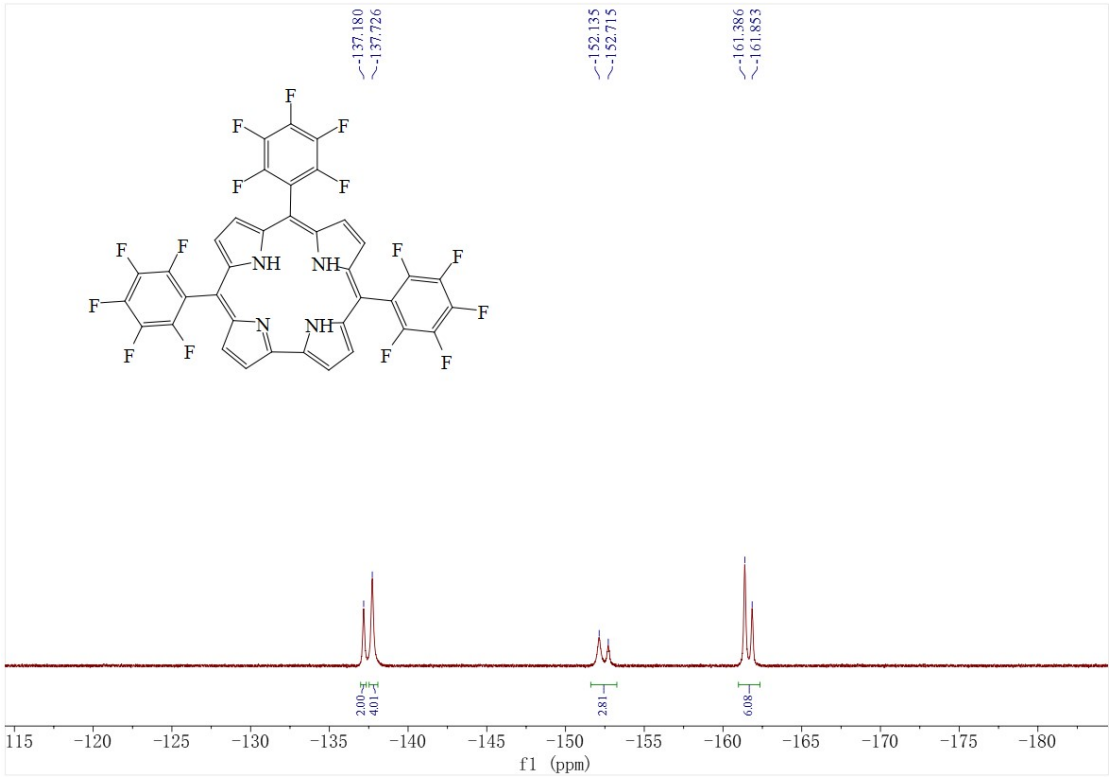

Fig. S3 ^{19}F NMR spectrum of $F_{15}C$.

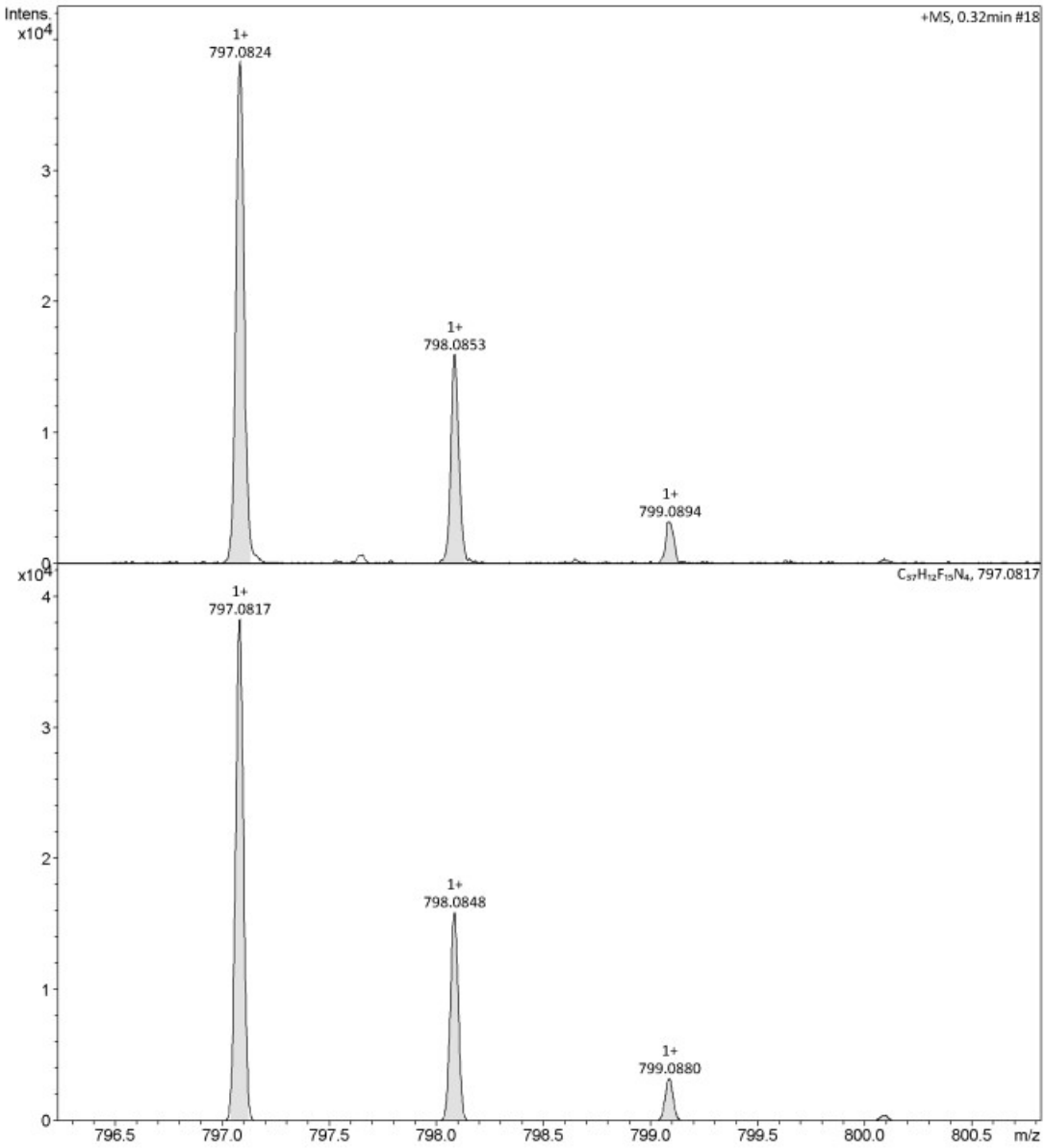

Fig. S4 ESI-HRMS spectrum of $F_{15}C$.

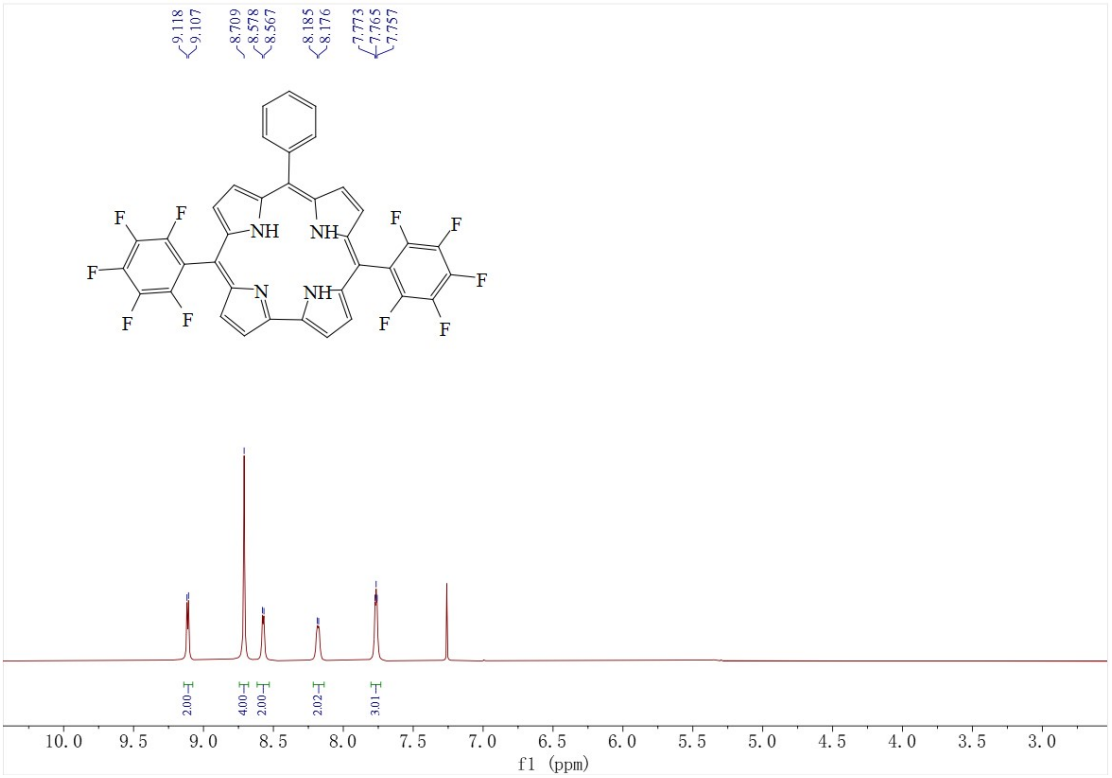

Fig. S5 ^{1}H NMR spectrum of $F_{10}C$.

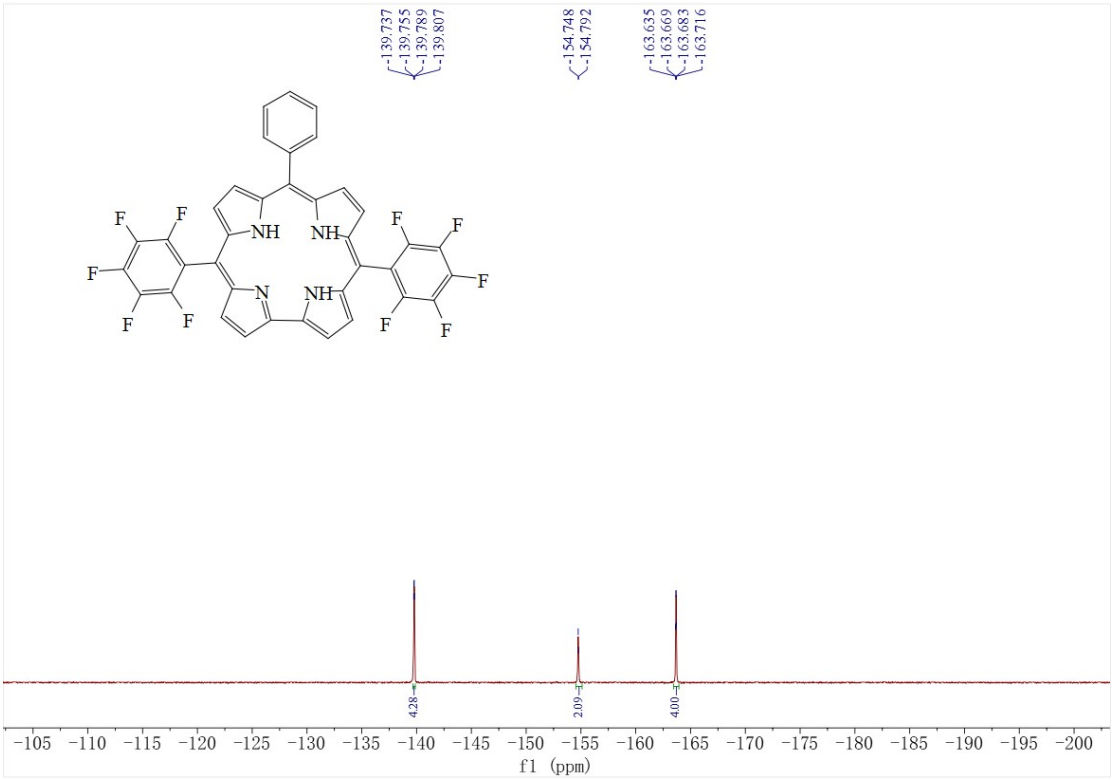

Fig. S6 ^{19}F NMR spectrum of $F_{10}C$.

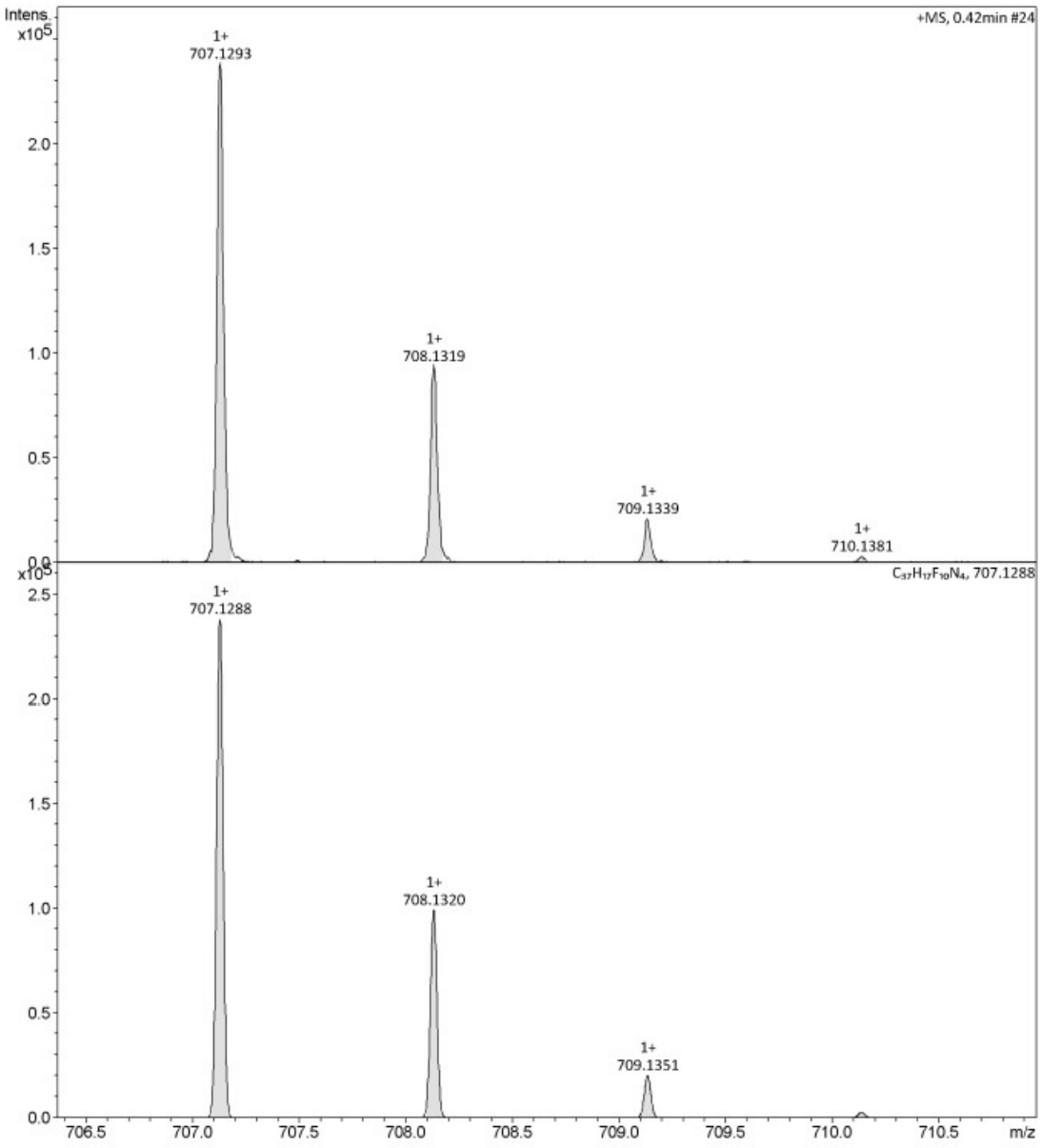

Fig. S7 ESI-HRMS spectrum of $F_{10}C$.

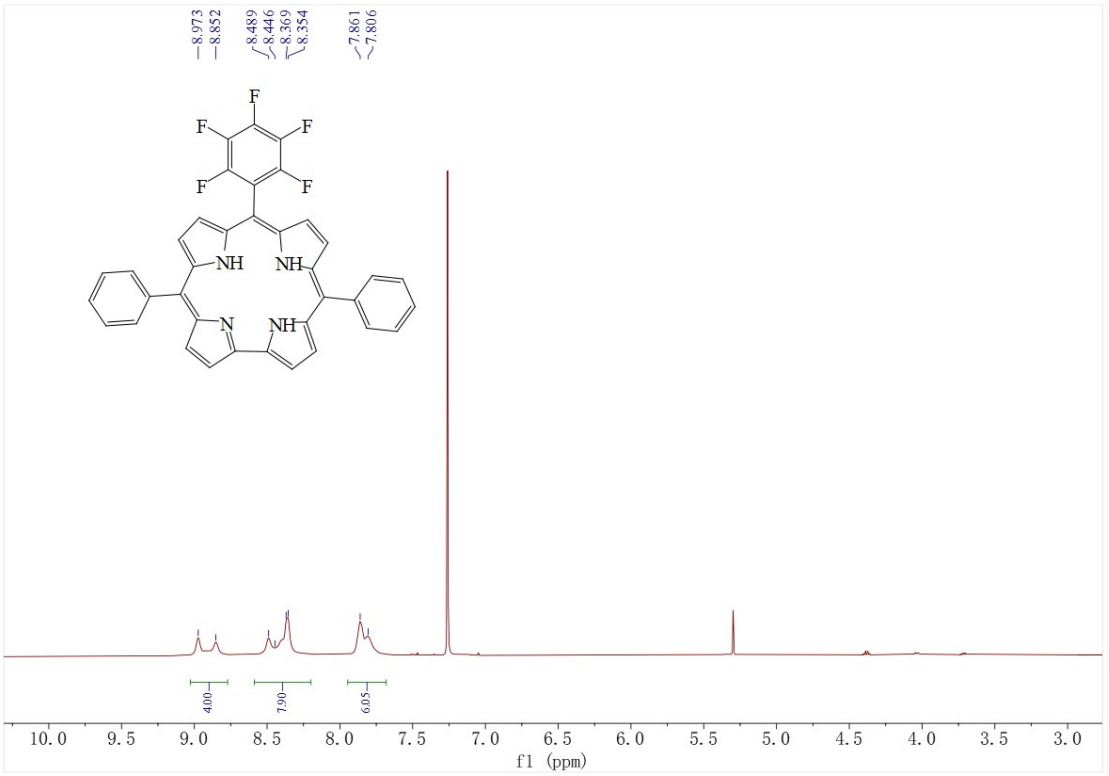

Fig. S8 ^{1}H NMR spectrum of F_5C.

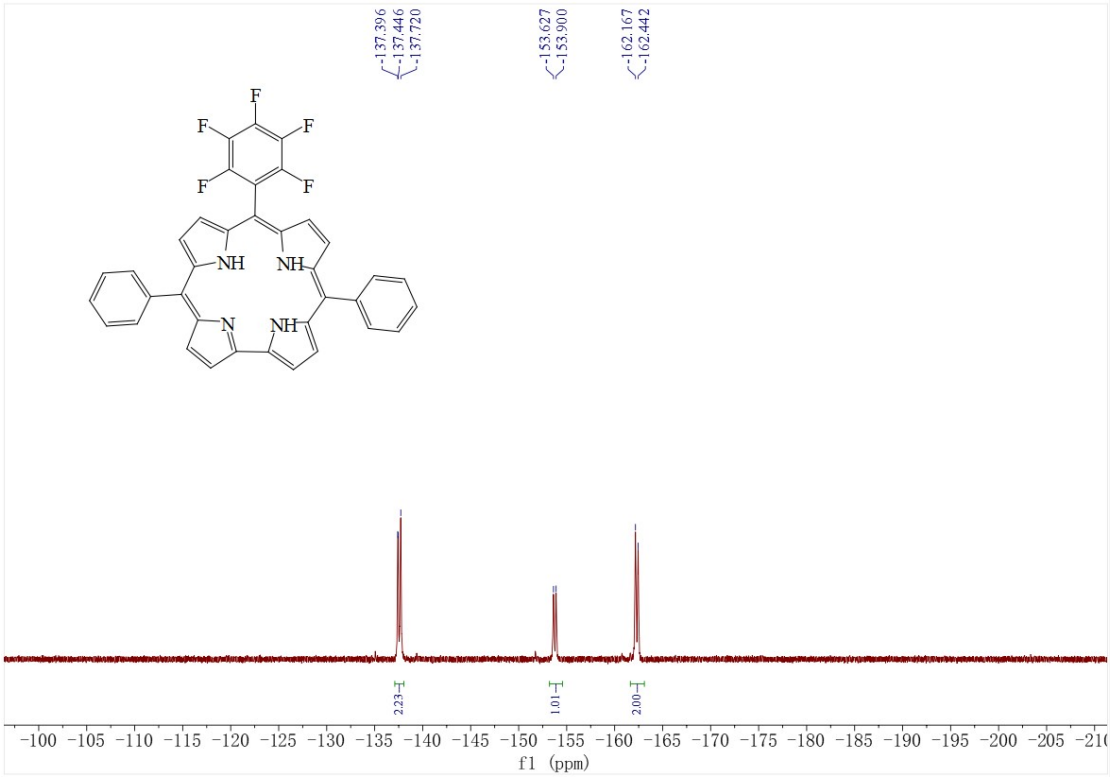

Fig. S9 ^{19}F NMR spectrum of F_5C.

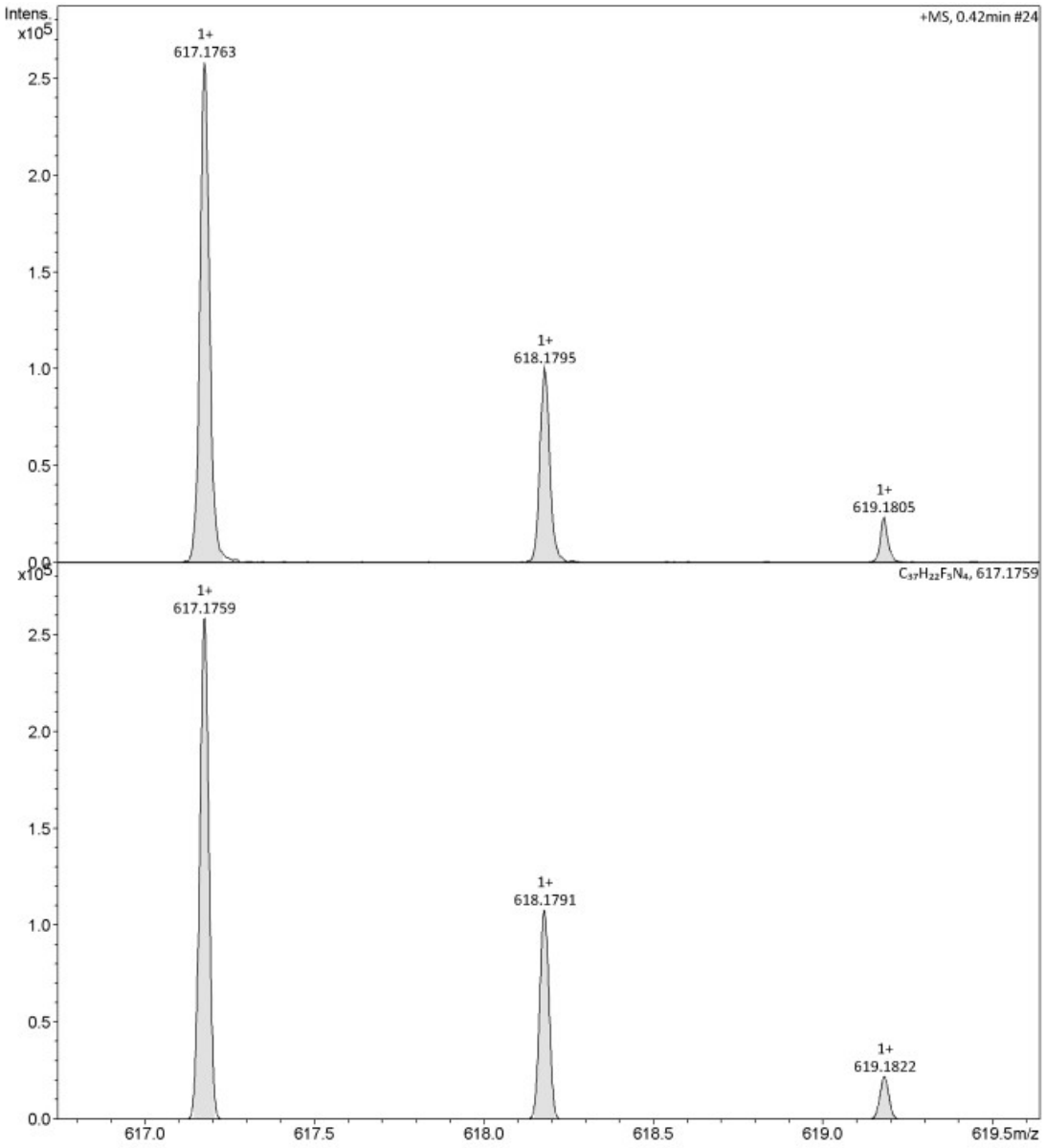

Fig. S10 ESI-HRMS spectrum of F_5C.

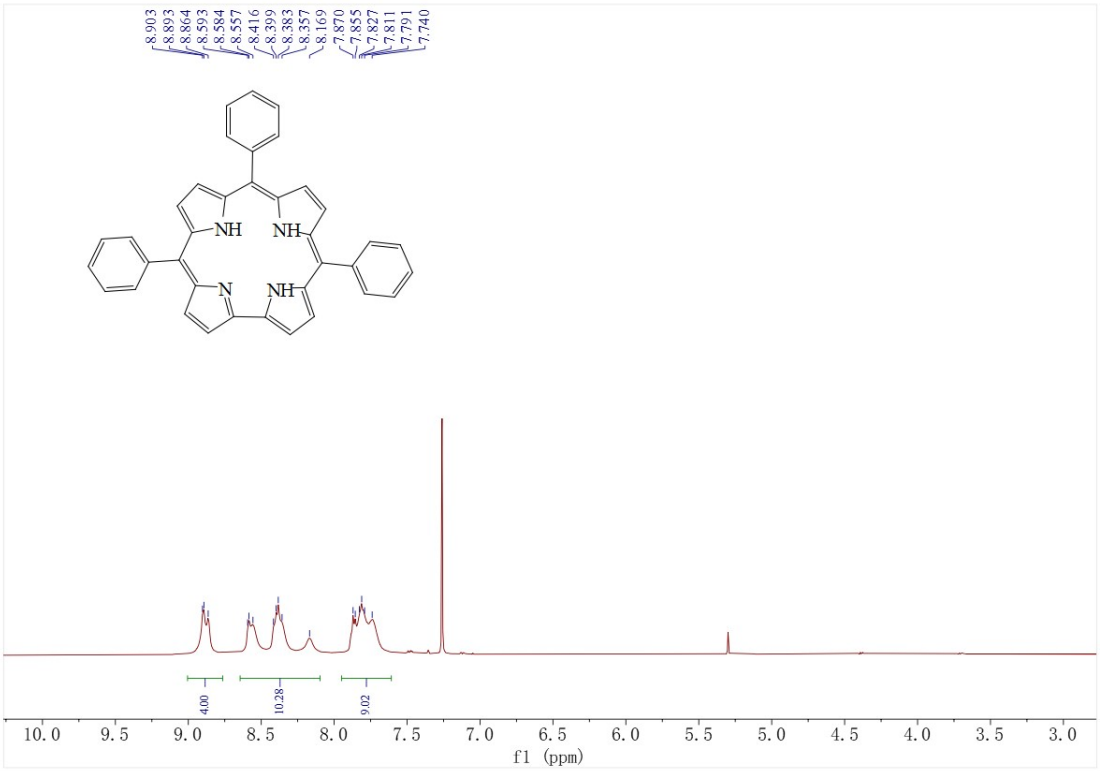

Fig. S11 ^{1}H NMR spectrum of F_0C.

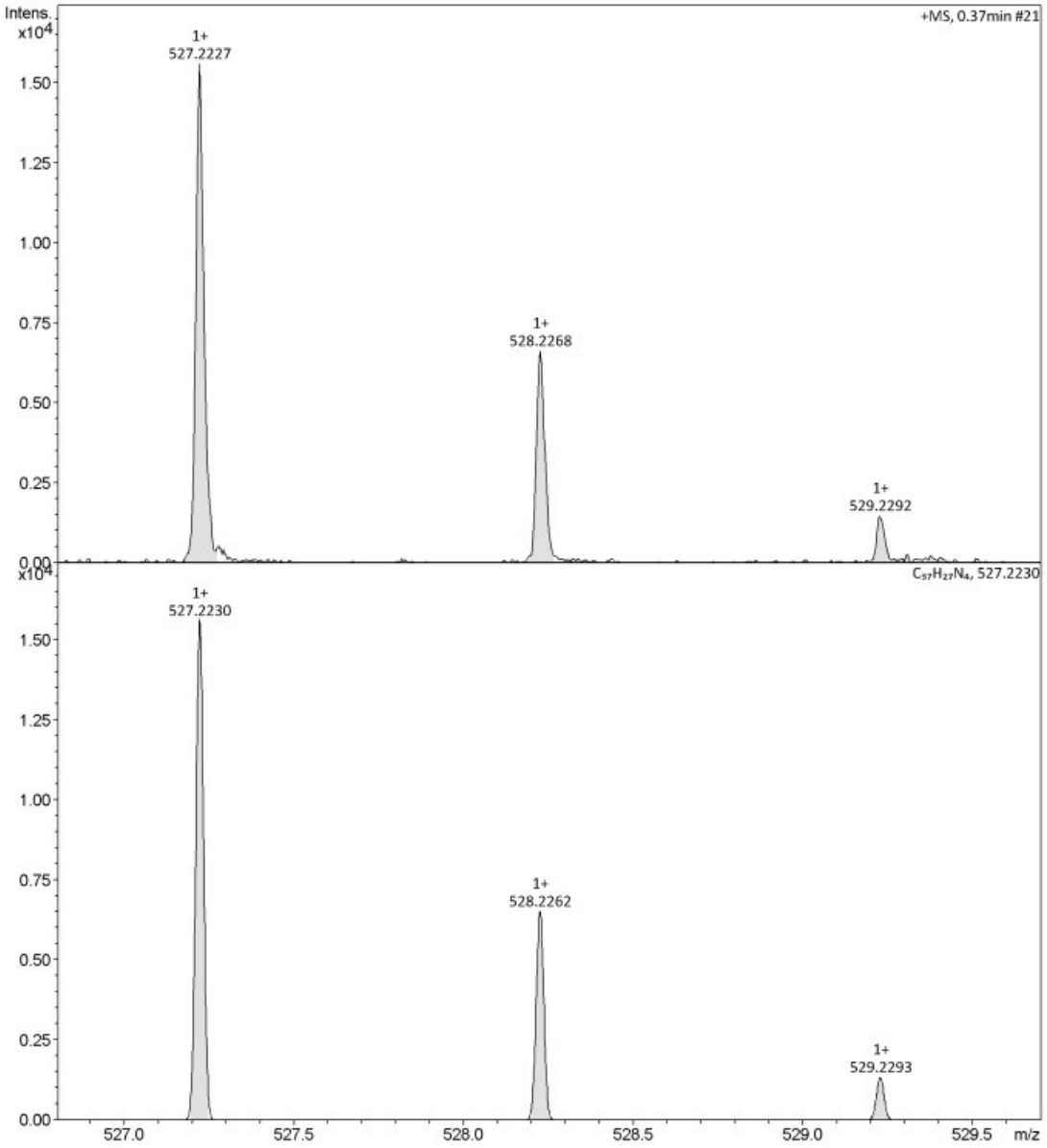

Fig. S12 ESI-HRMS spectrum of F_0C.

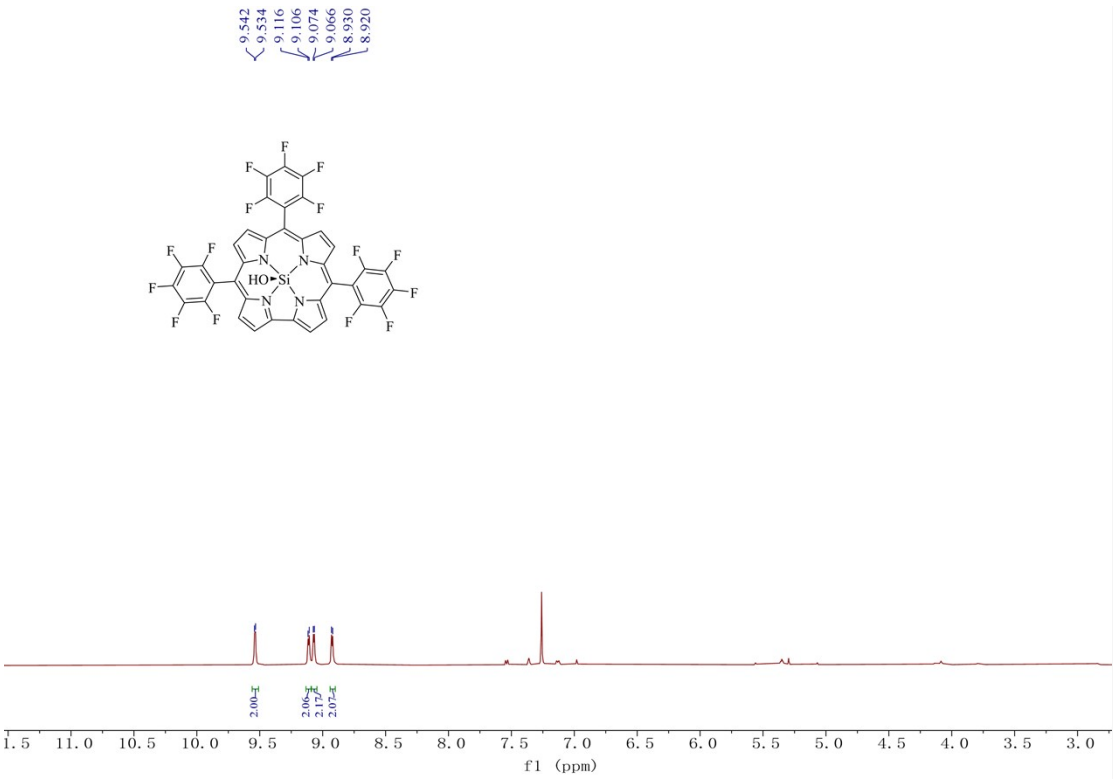

Fig. S13 ^{1}H NMR spectrum of F_{15}C-Si.

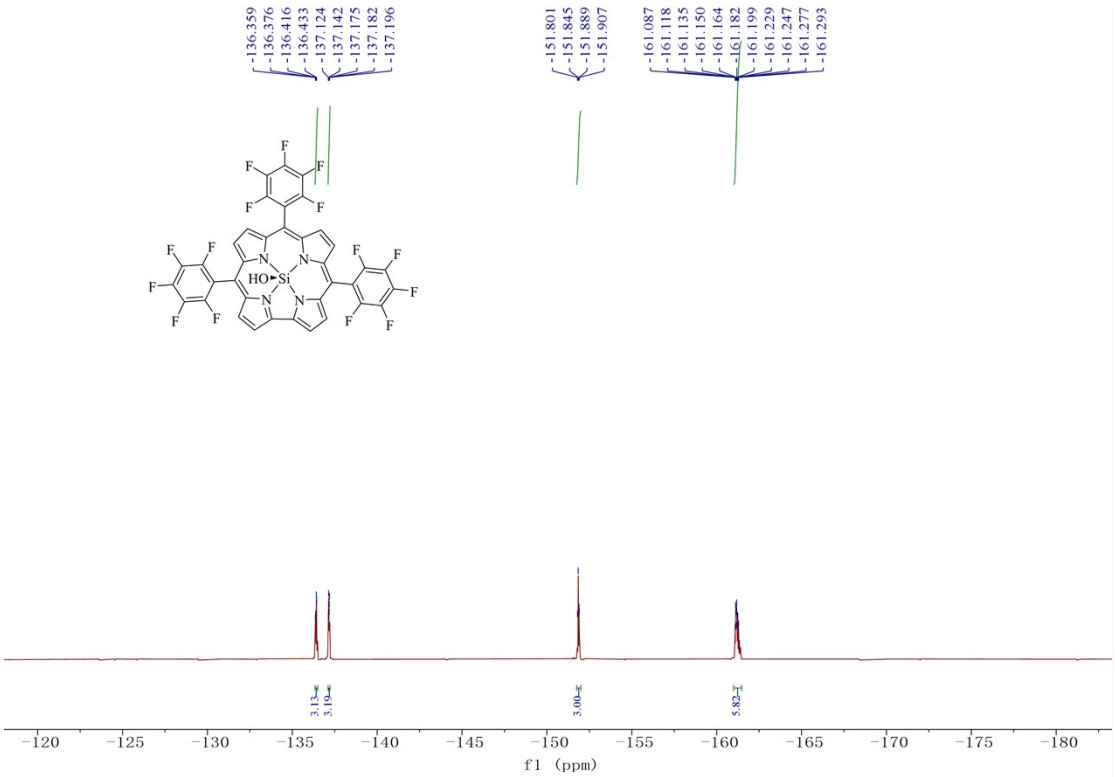

Fig. S14 ^{19}F NMR spectrum of F_{15}C-Si.

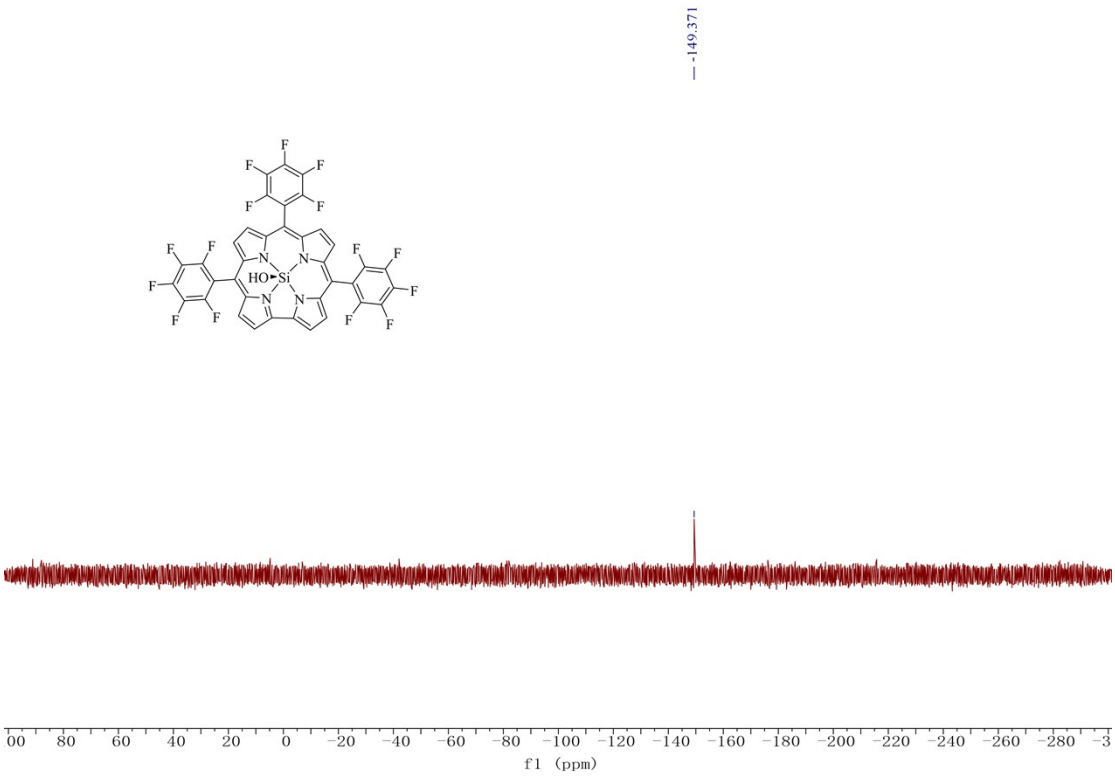

Fig. S15 ^{29}Si NMR spectrum of F_{15}C-Si.

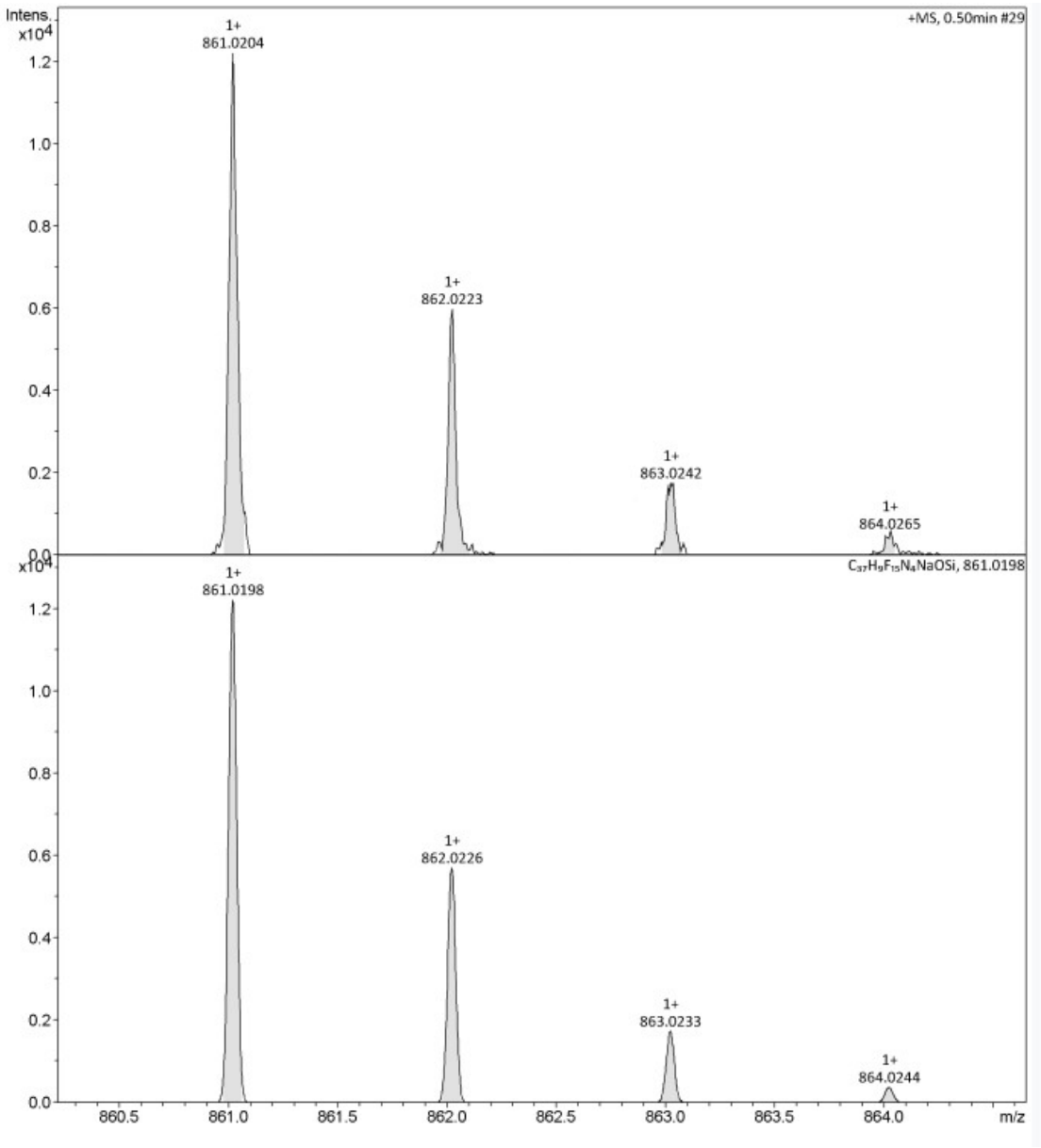

Fig. S16 ESI-HRMS spectrum of F_{15}C-Si.

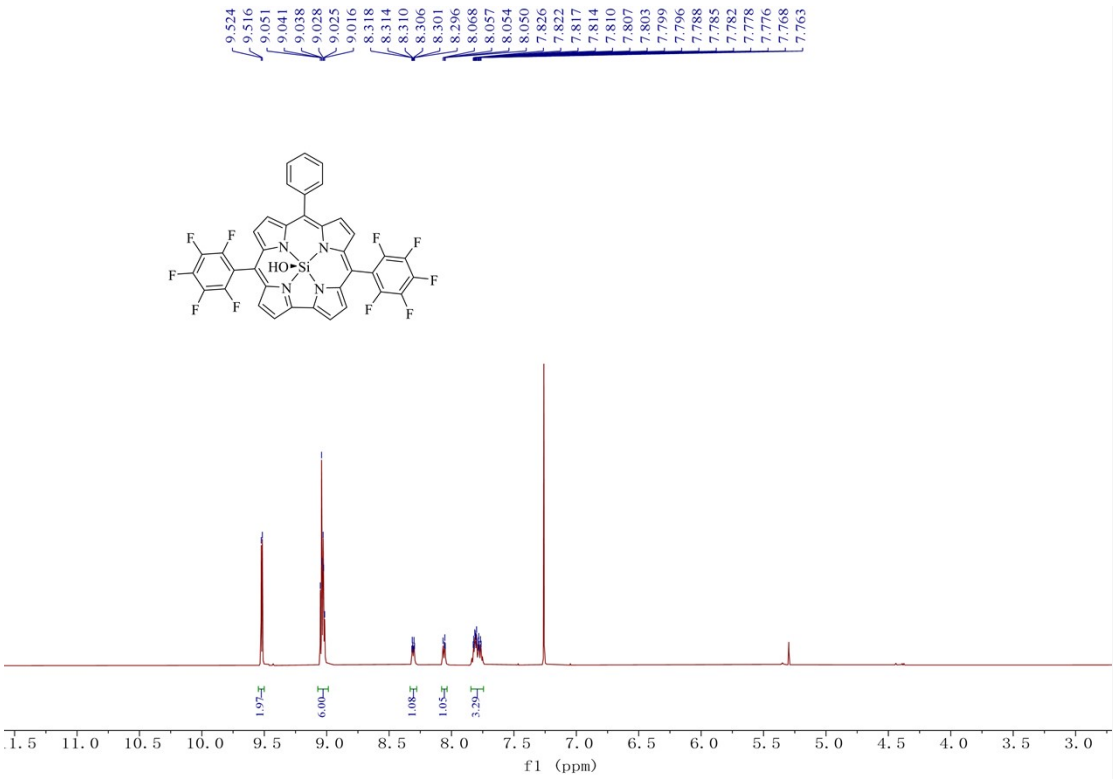

Fig. S17 ^{1}H NMR spectrum of F_{10}C-Si.

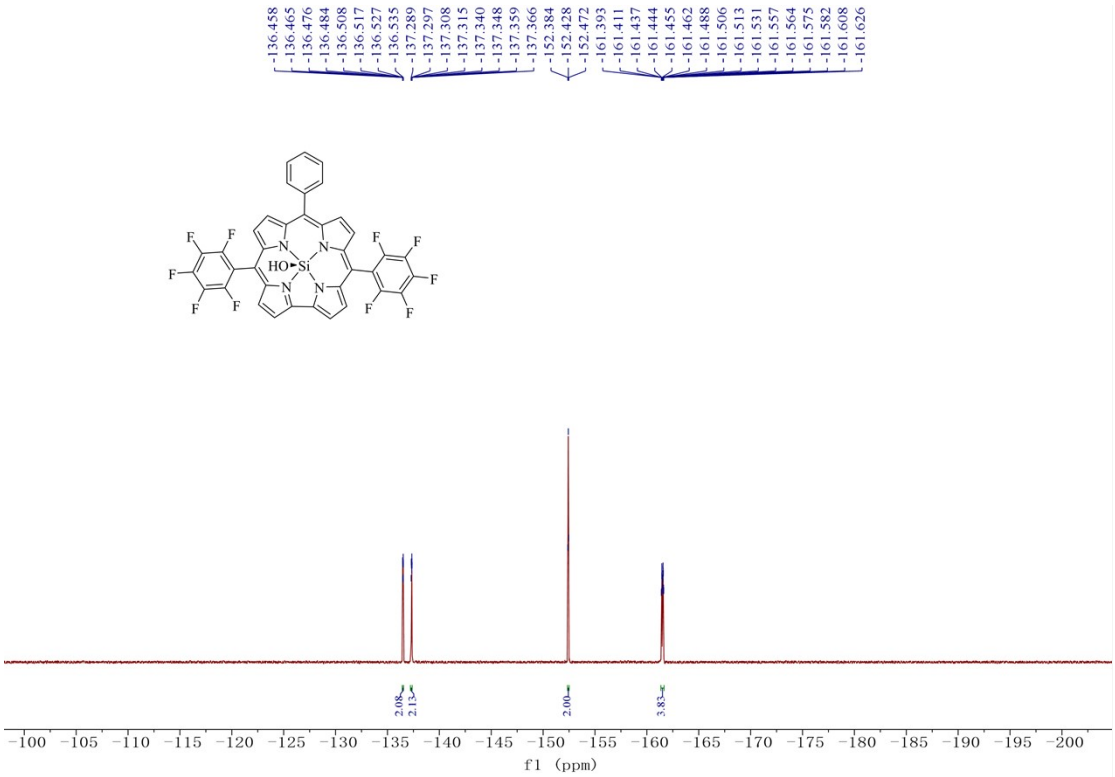

Fig. S18 ^{19}F NMR spectrum of F_{10}C-Si.

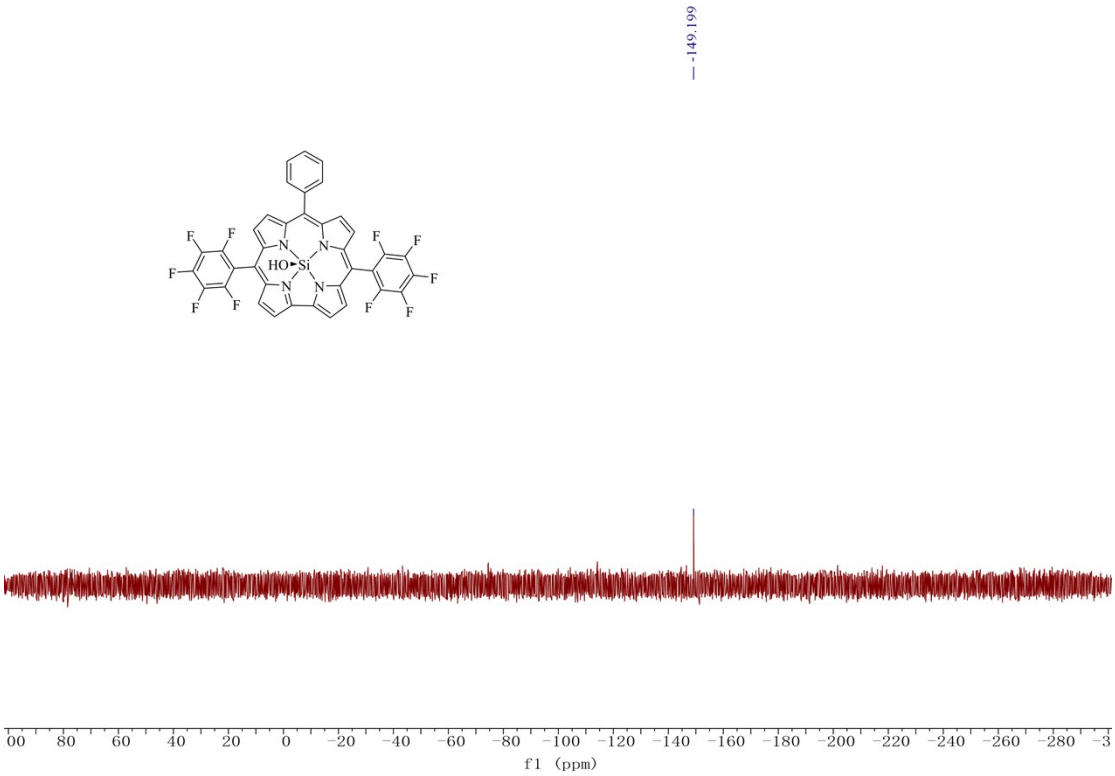

Fig. S19 ^{29}Si NMR spectrum of F_{10}C-Si.

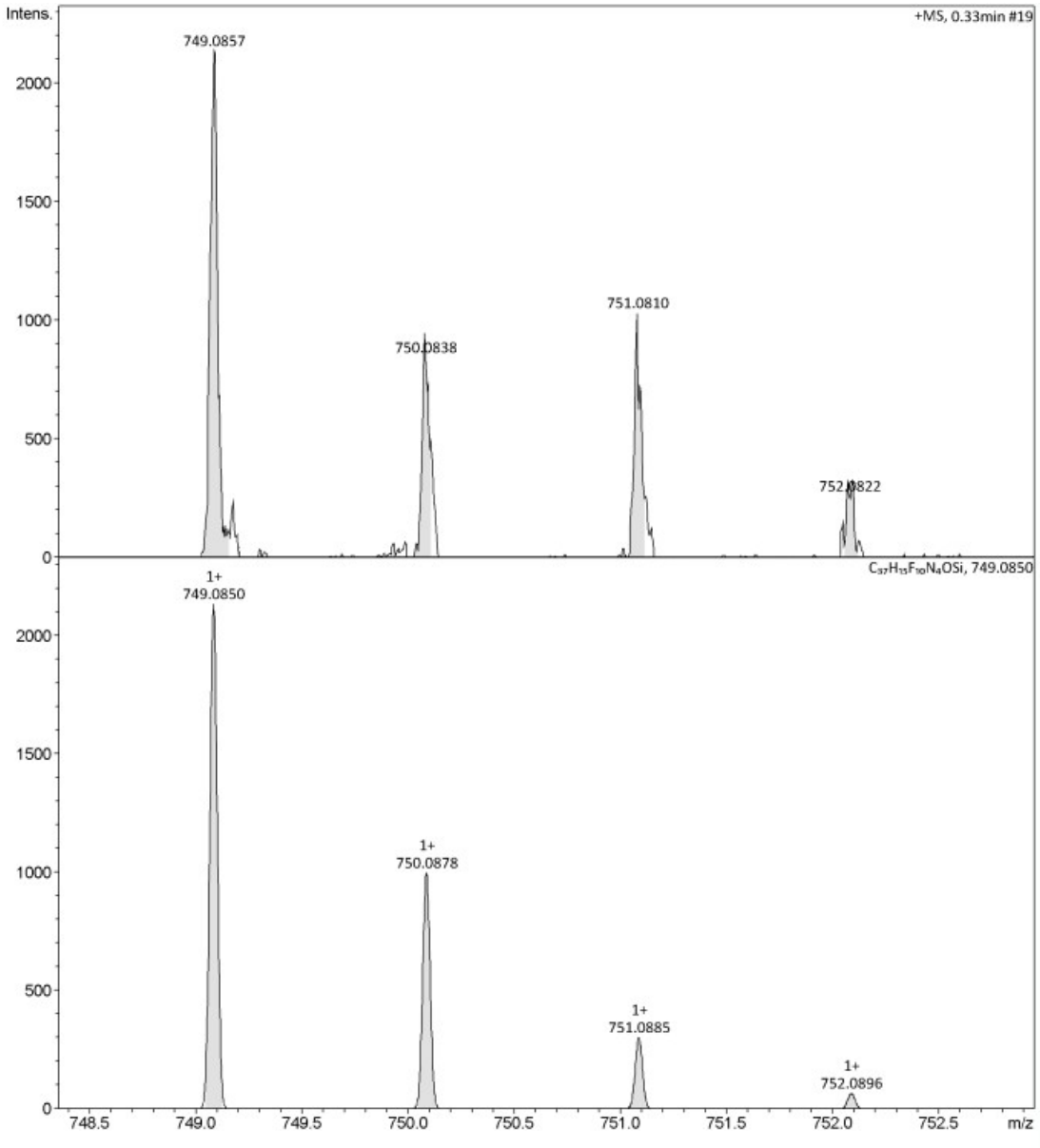

Fig. S20 ESI-HRMS spectrum of F_{10}C-Si.

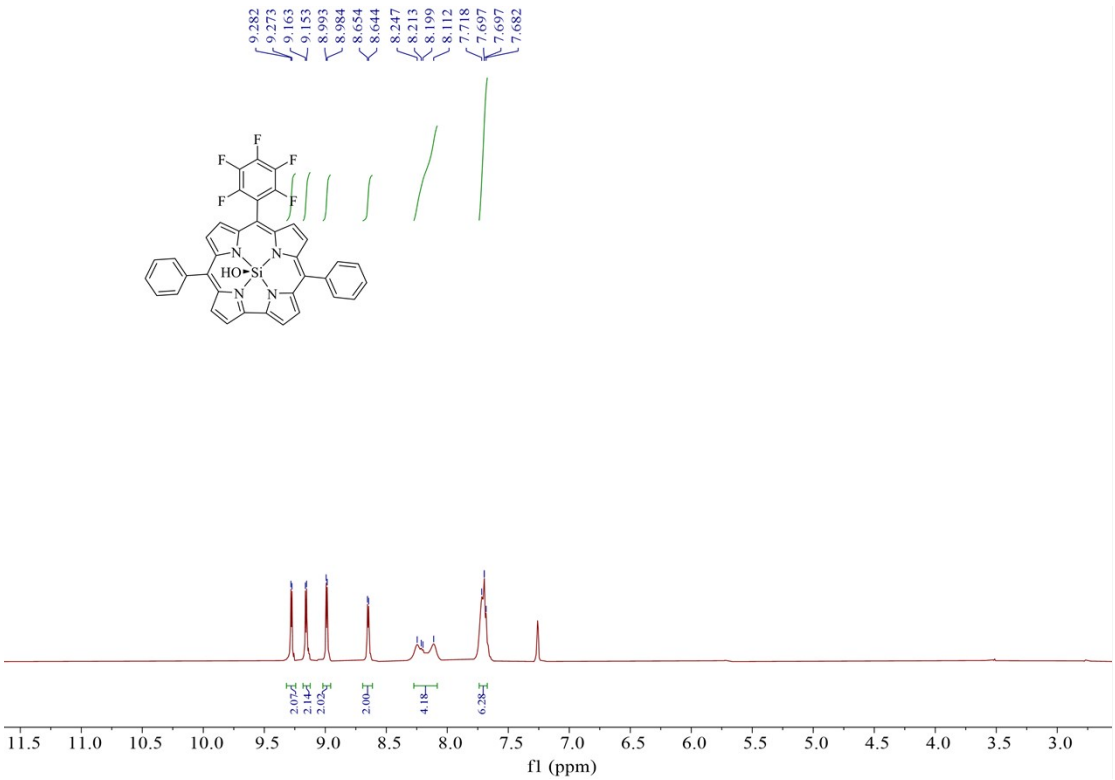

Fig. S21 ^{1}H NMR spectrum of F_5C-Si.

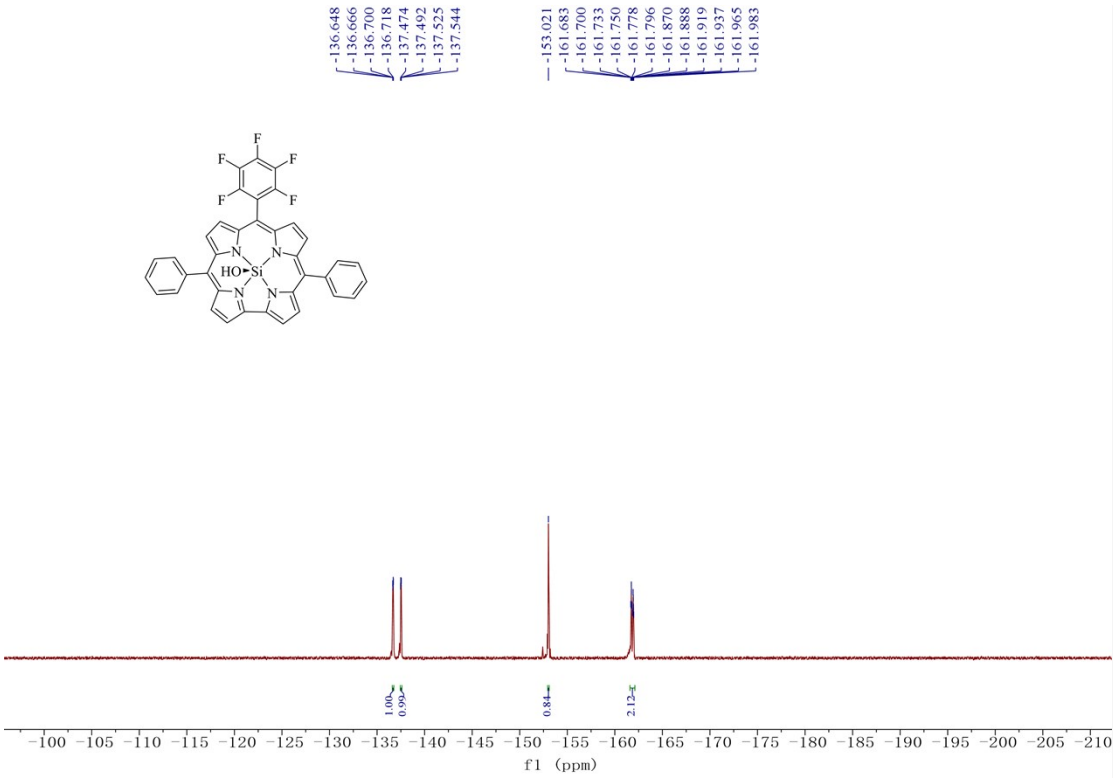

Fig. S22 ^{19}F NMR spectrum of F_5C-Si.

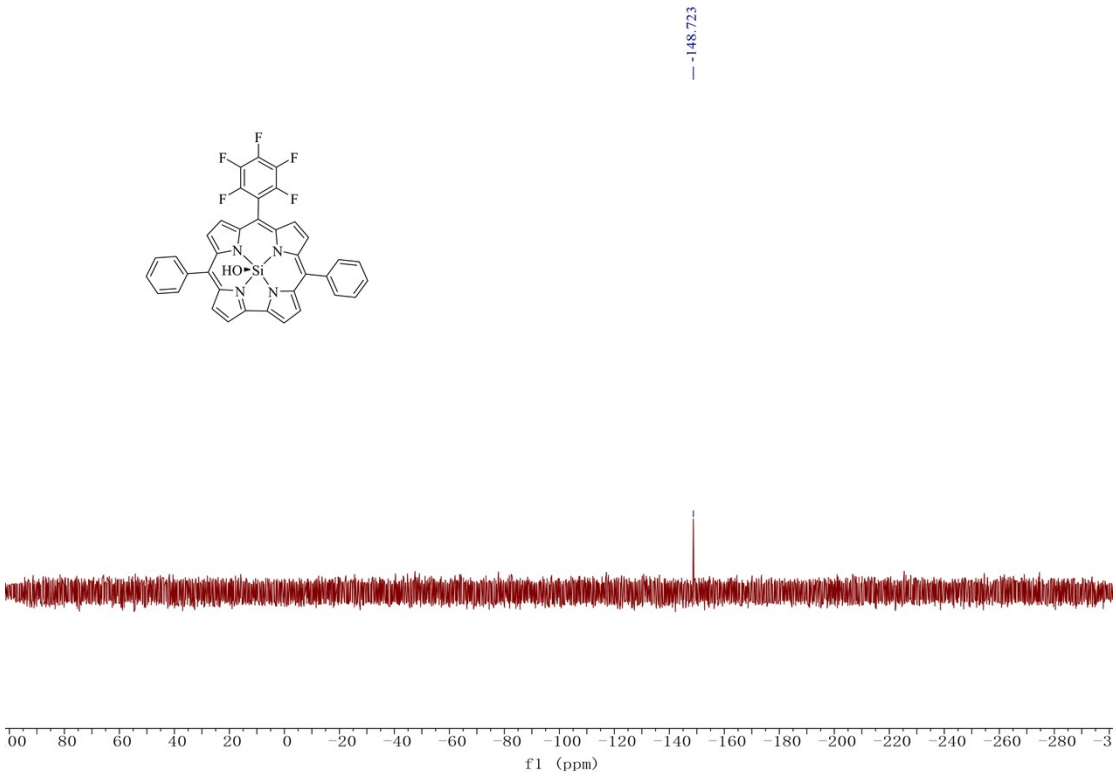

Fig. S23 ^{29}Si NMR spectrum of F_5C-Si.

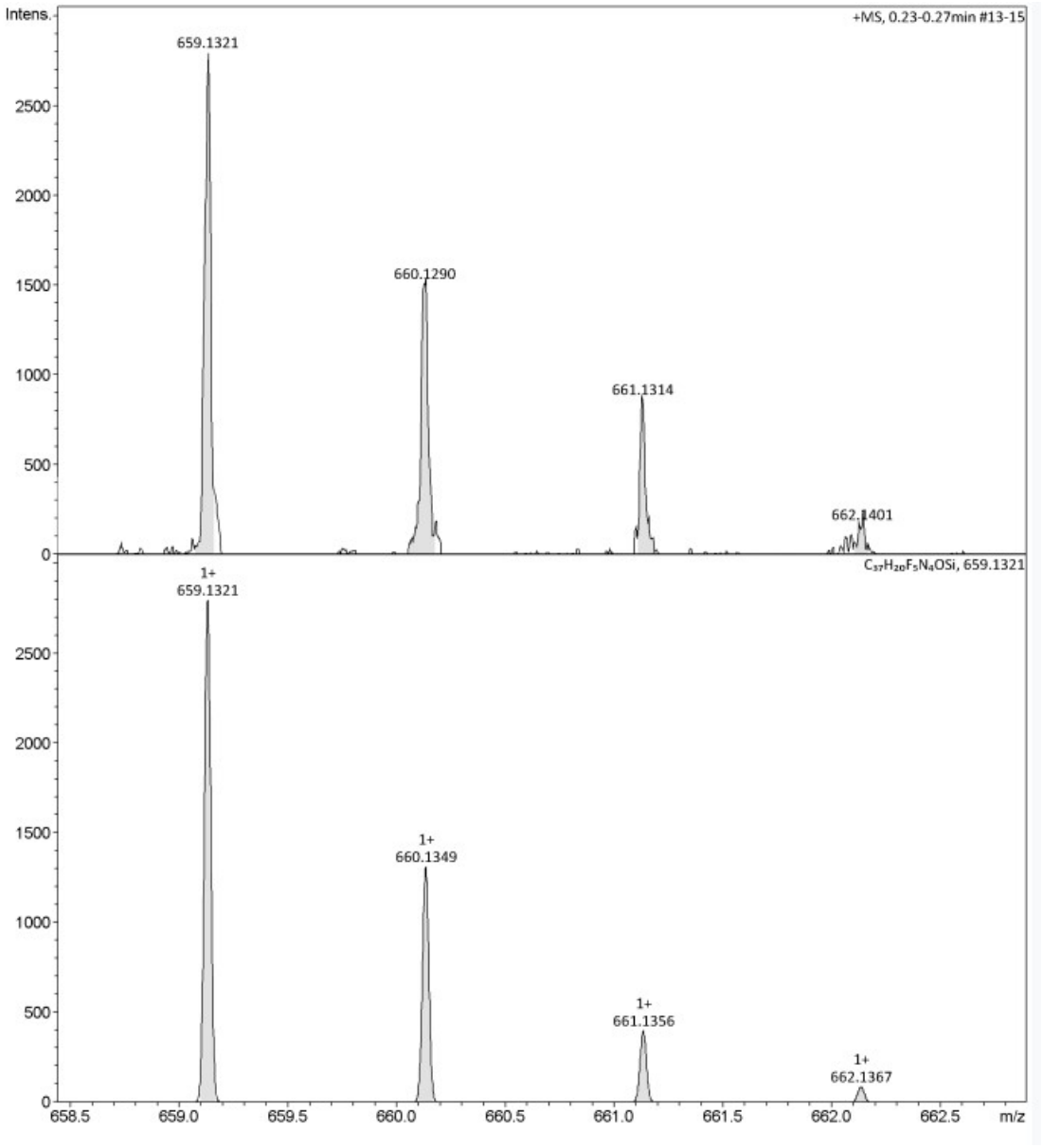

Fig. S24 ESI-HRMS spectrum of F_5C-Si.

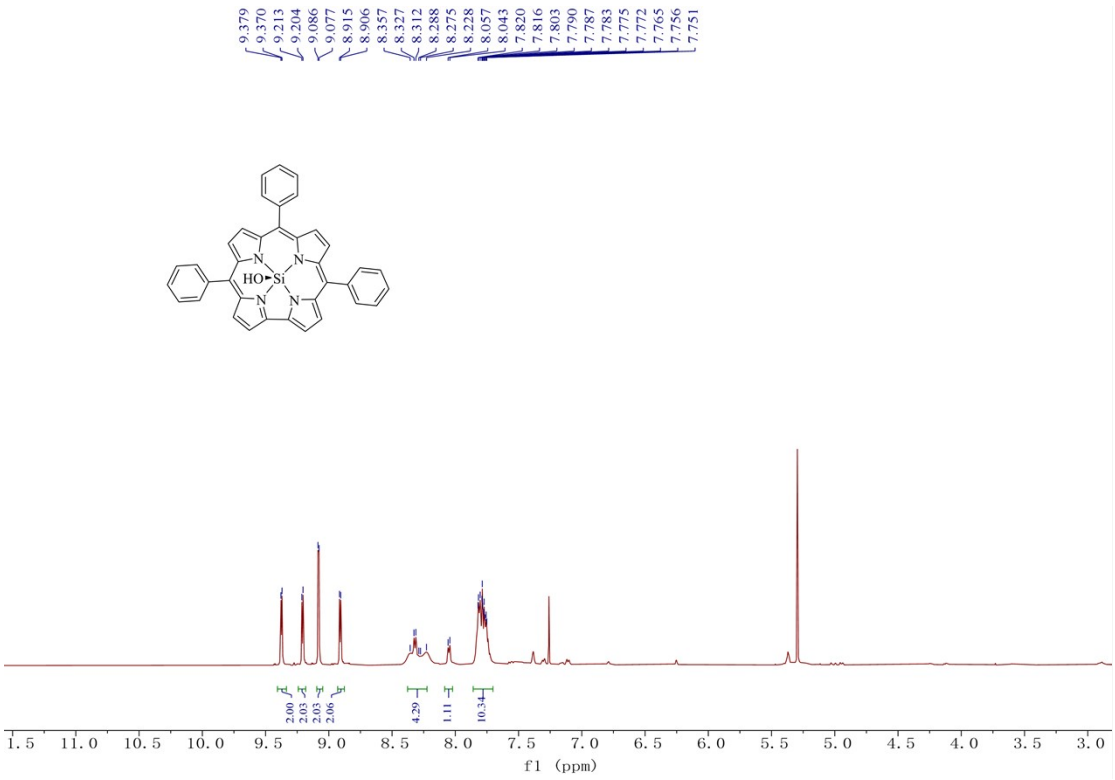

Fig. S25 ^{1}H NMR spectrum of F_0C-Si.

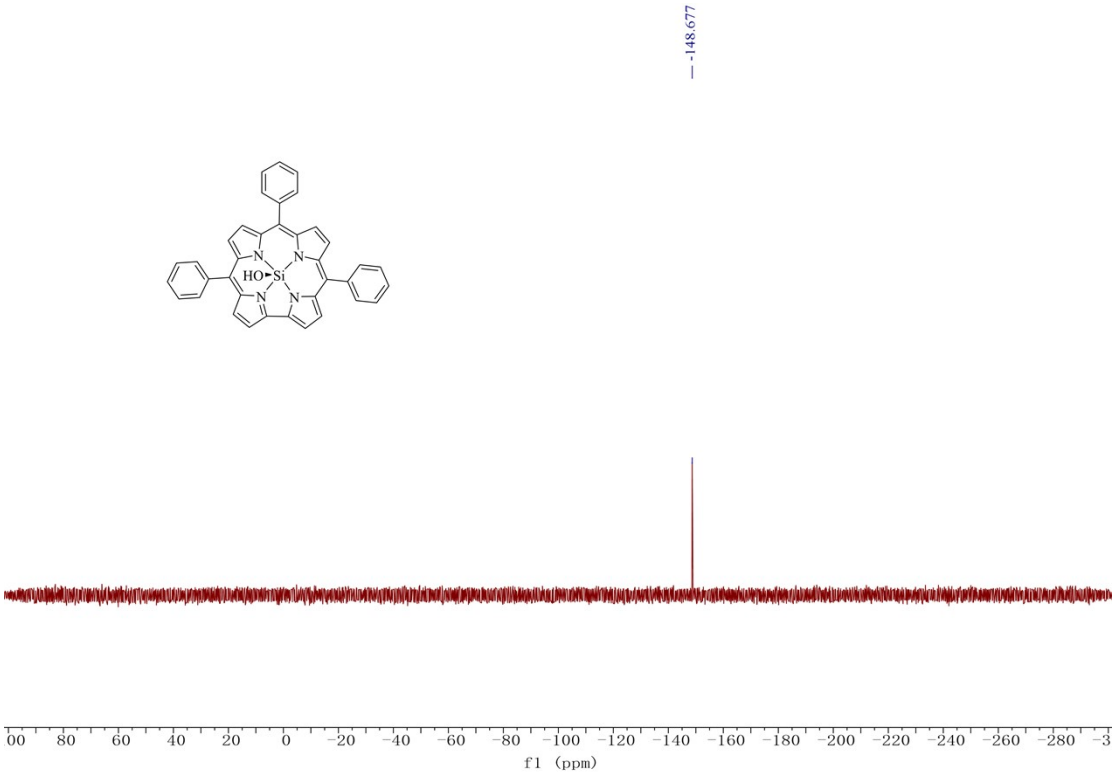

Fig. S26 ^{29}Si NMR spectrum of F_0C-Si.

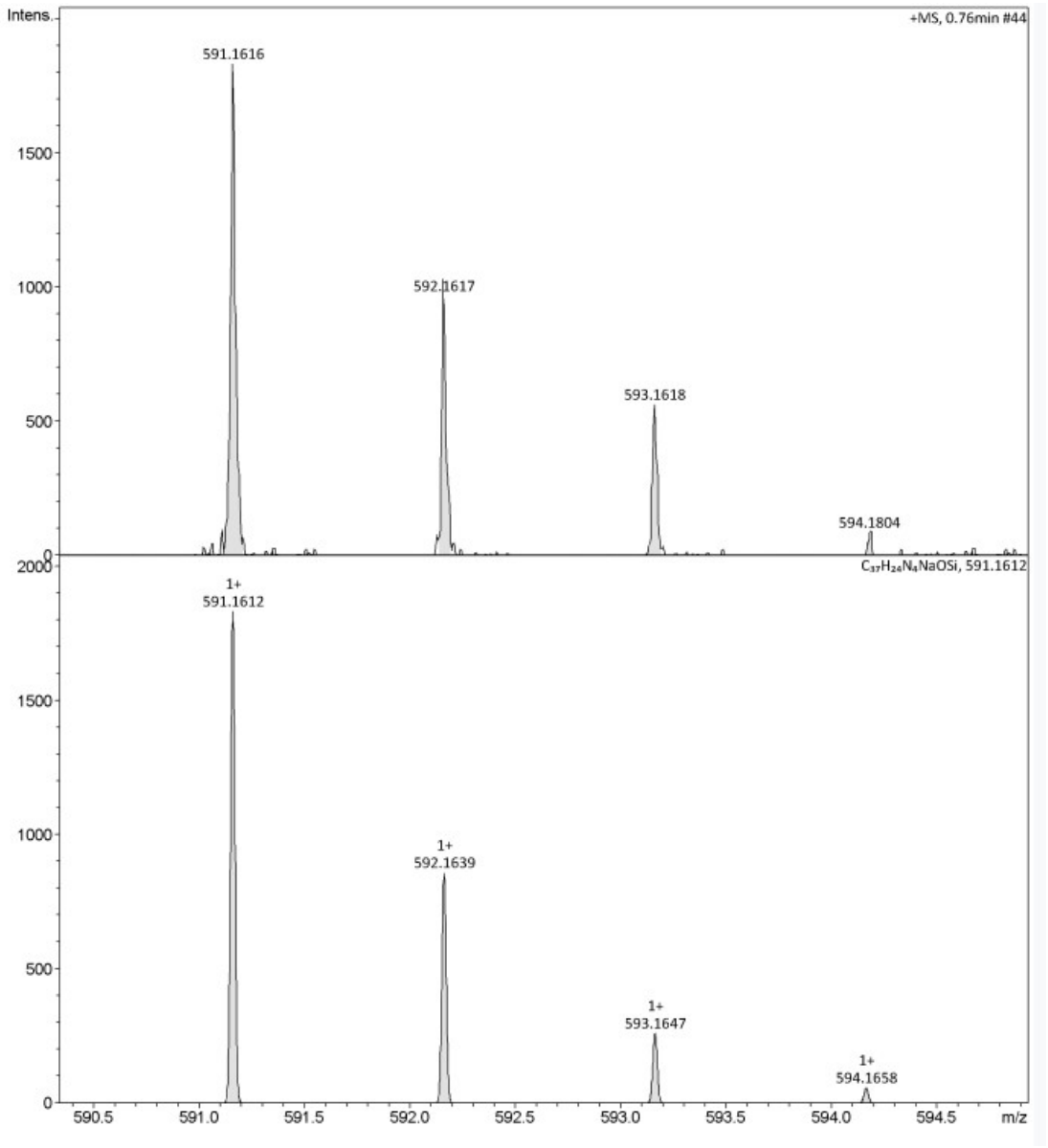

Fig. S27 ESI-HRMS spectrum of F_0C-Si.

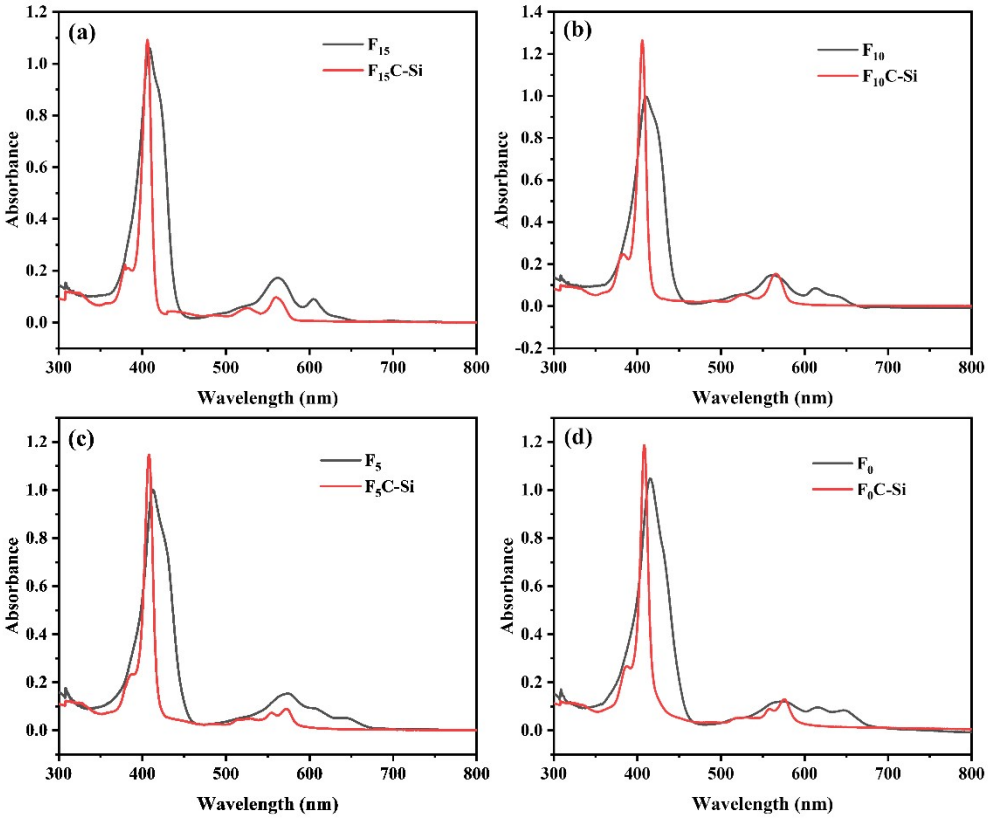

Fig. S28 UV-vis spectra of $F_{15}C$ and $F_{15}C$-Si (a), $F_{10}C$ and $F_{10}C$-Si (b), F_5C and F_5C-Si (c), F_0C and F_0C-Si (d) in CH_2Cl_2 solvent at room temperature.

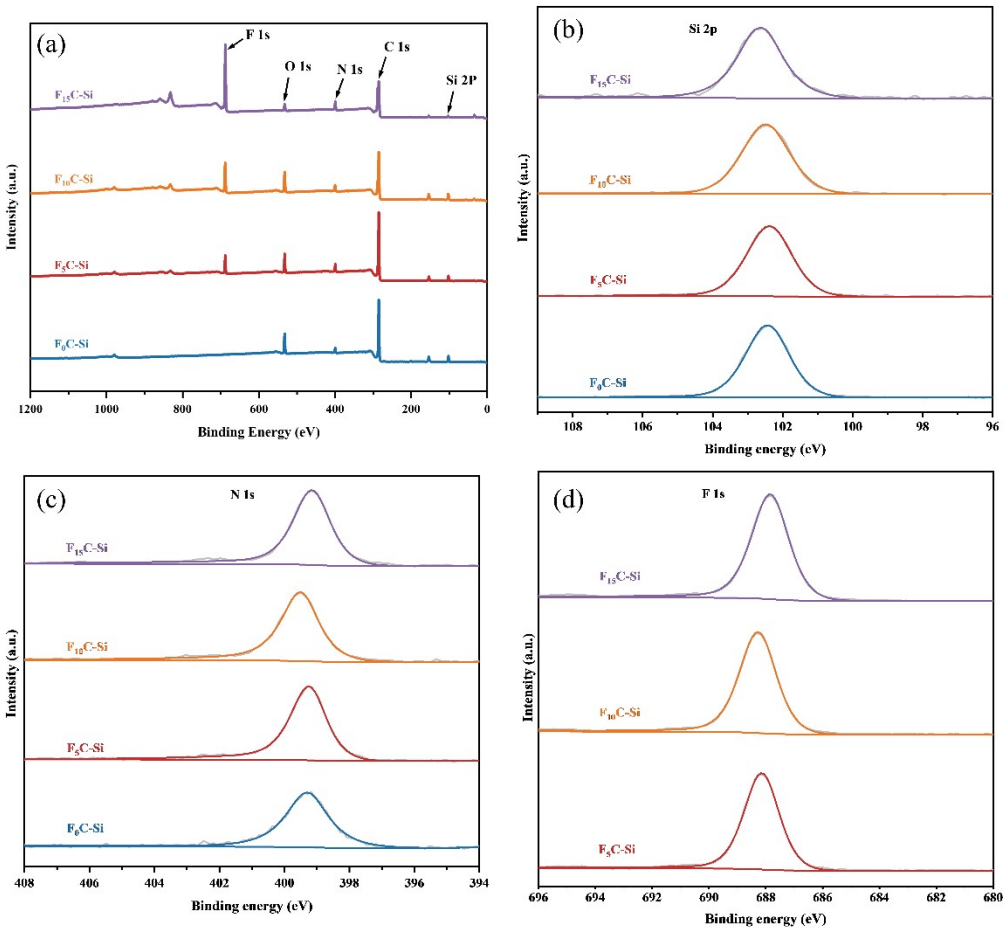

Fig. S29 XPS survey scan spectra of F_{15}C-Si, F_{10}C-Si, F_5C-Si and F_0C-Si and high-resolution XPS of characteristic element, a) full spectrum b) Si 2p c) N 1s d) F 1s.

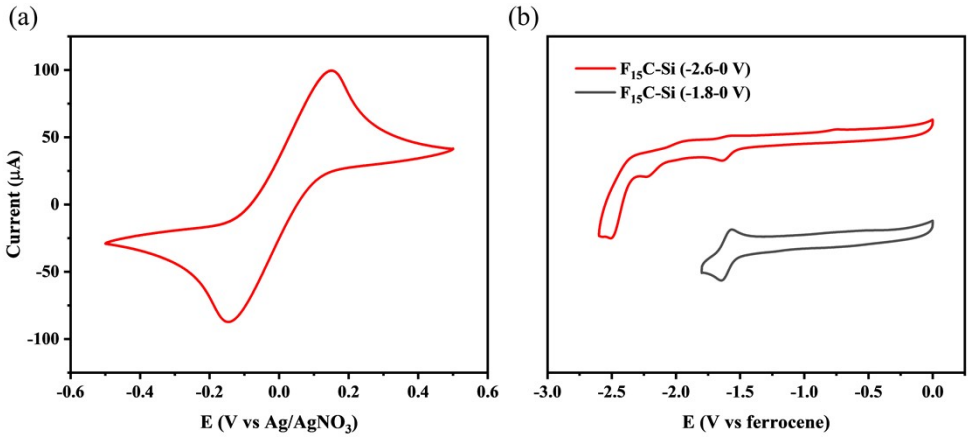

Fig. S30 (a) The redox couple of ferrocene in DMF containing 0.10 M TBAP with blank glassy carbon as the working electrode; (b) CVs of F_{15}C-Si in the range of -2.6 - 0 V and -1.8 - 0 V in N_2-saturated DMF containing 0.10 M TBAP.

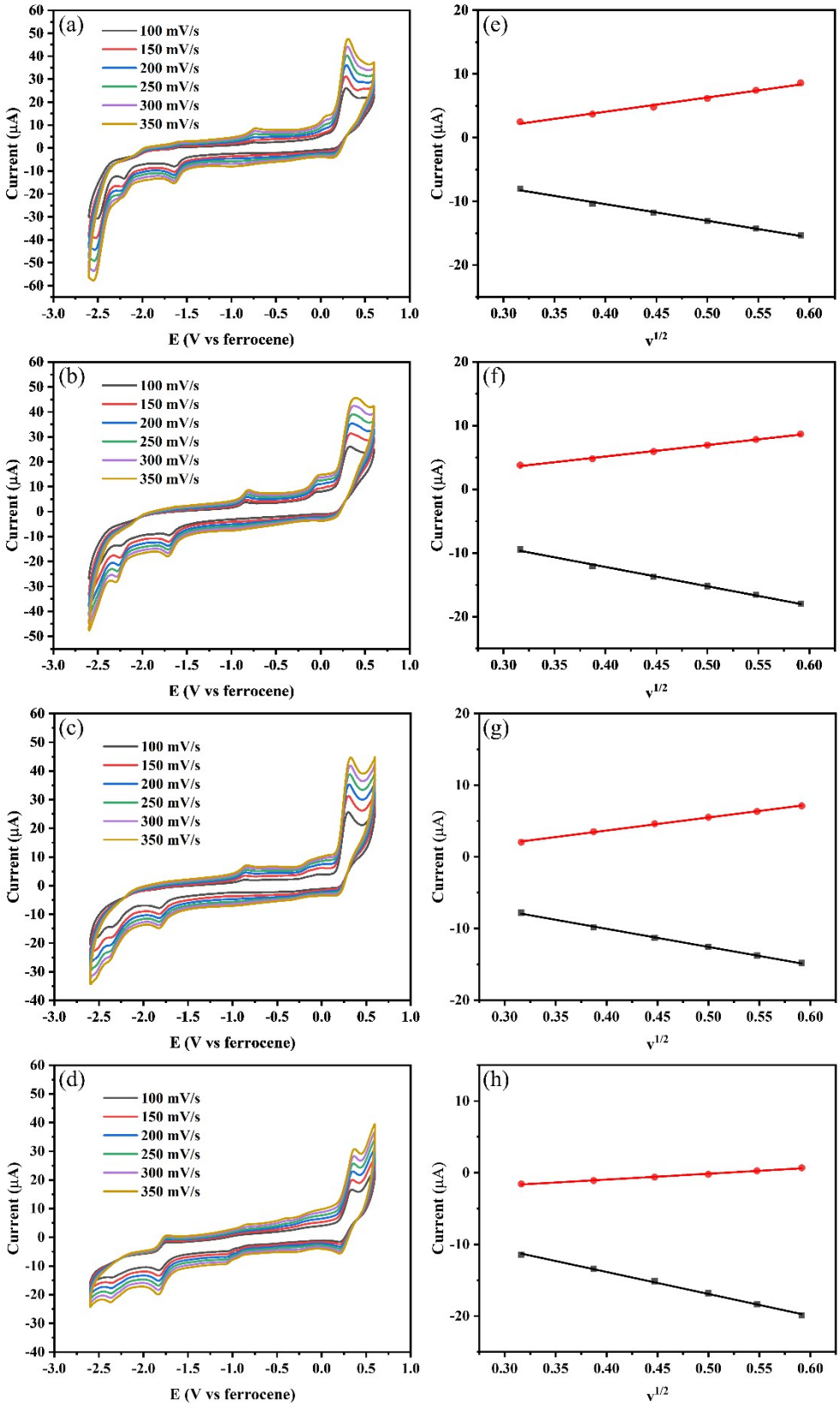

Fig. S31 CVs of 0.5 mM (a) F_{15}C-Si, (b) F_{10}C-Si, (c) F_5C-Si and (d) F_0C-Si with a varying scan rate (υ) from 50 mV/s to 350 mV/s using the glassy carbon as the working electrode and plots of the maximum current (i_p) for the reduction and oxidation waves vs. the scan rate ($\upsilon^{1/2}$) (e-h).

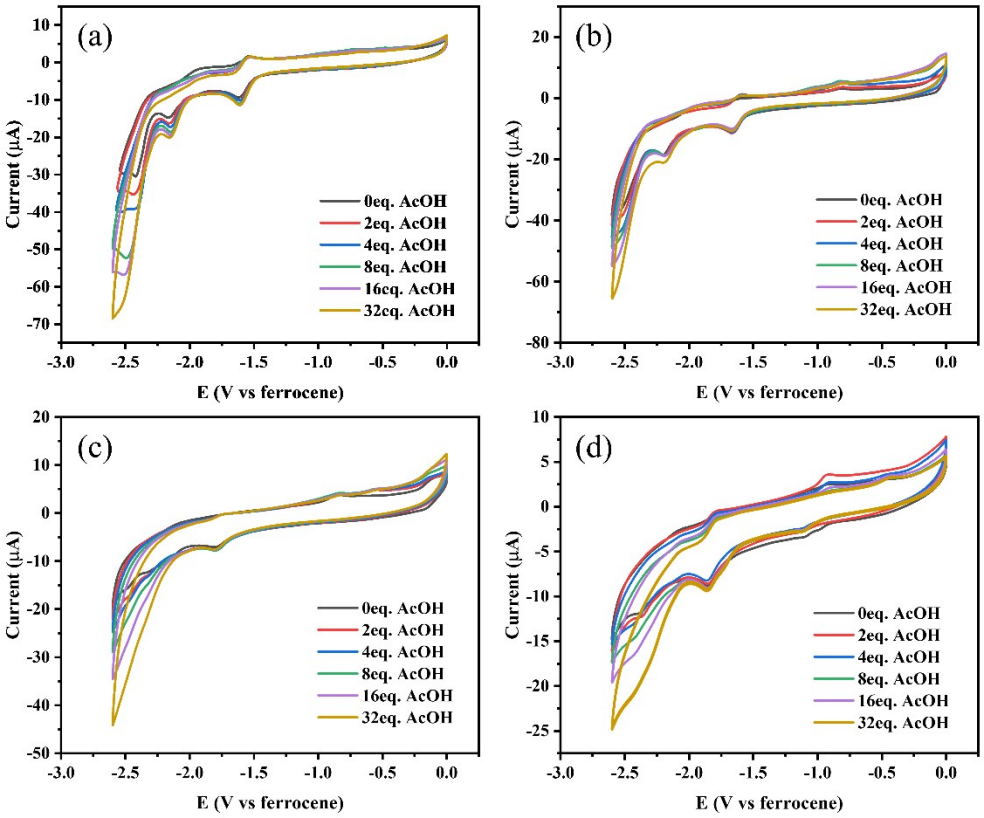

Fig. S32 CVs of 0.5 mM silicon corrole complexes (F_{15}C-Si to F_0C-Si) (a-d) with increasing amounts of AcOH from 0 to 32 equivalents in N_2-saturated DMF containing 0.1 M TBAP.

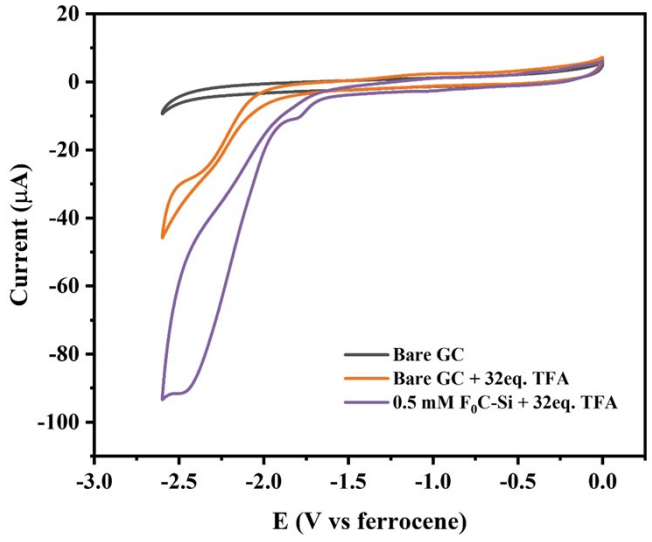

Fig. S33 CVs of bare glassy carbon electrode and 0.5 mM F_0C-Si in DMF containing 0.1 M TBAP with 32 equivalents TFA.

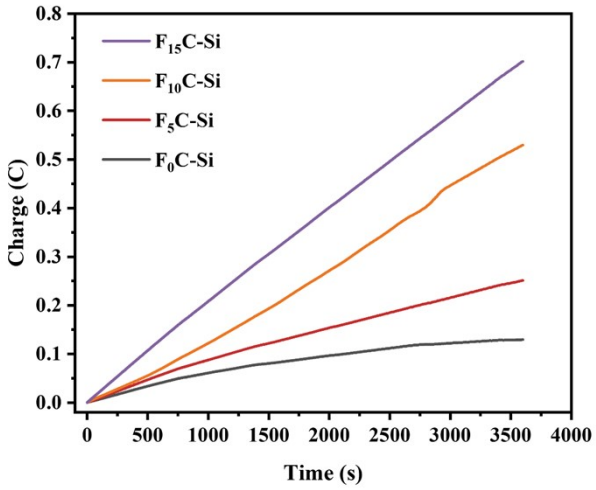

Fig. S34 Charge of 0.5 mM F_{15}C-Si, F_{10}C-Si, F_5C-Si and F_0C-Si after 1 h of electrolysis in DMF containing 0.1 M TBAP with 32 equivalents TFA.

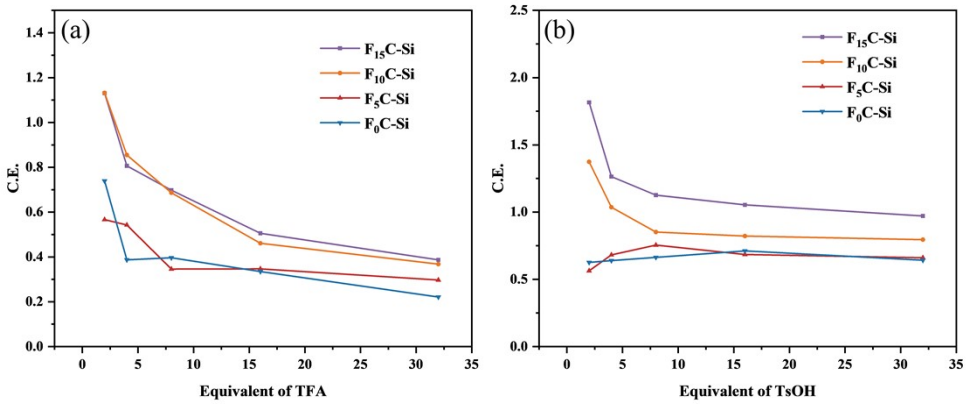

Fig. S35 The variation of C.E. for F_{15}C-Si, F_{10}C-Si, F_5C-Si and F_0C-Si under different concentrations of proton sources: a) TFA; b) TsOH.

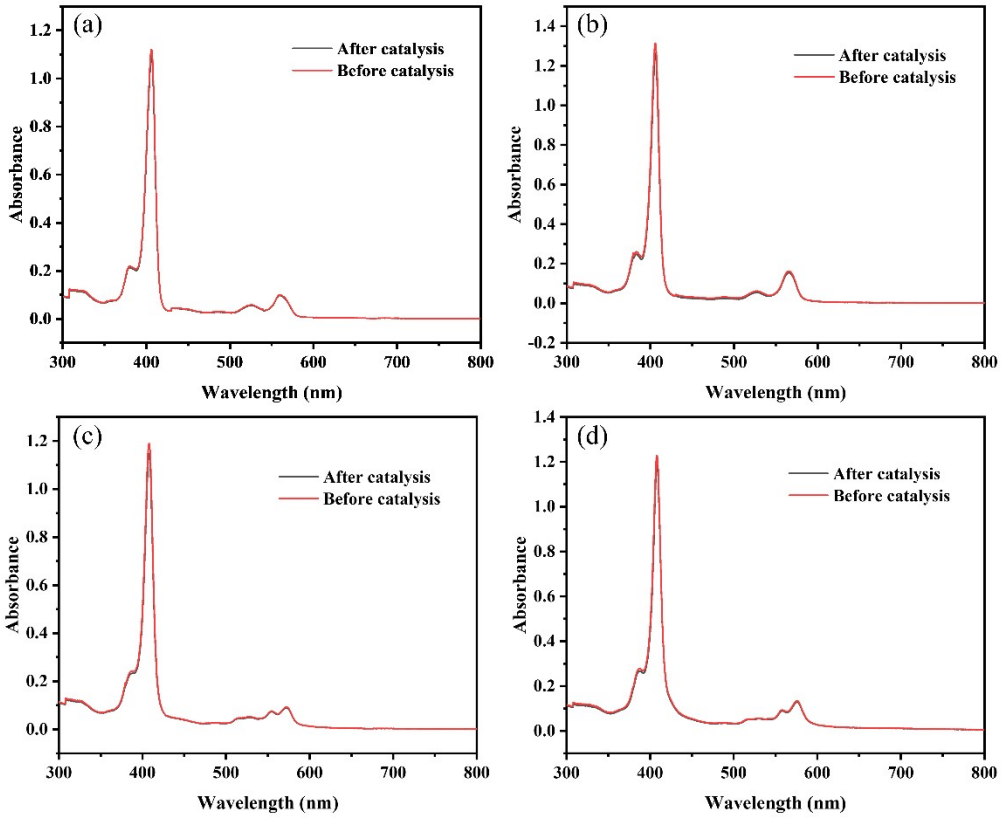

Fig. S36 UV-vis spectra of 0.5 mM F_{15}C-Si, F_{10}C-Si, F_5C-Si and F_0C-Si in DMF containing 0.1 M TBAP with 32 equivalents TFA and after 1 h electrolysis.

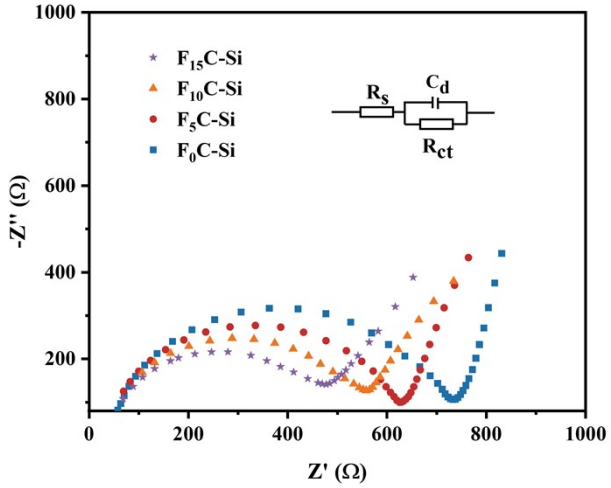

Fig. S37 The impedance plots of 0.5 mM F_{15}C-Si, F_{10}C-Si, F_5C-Si and F_0C-Si after one hour of electrolysis in DMF containing 0.1 M TBAP with the addition of 32 equivalents of TFA.

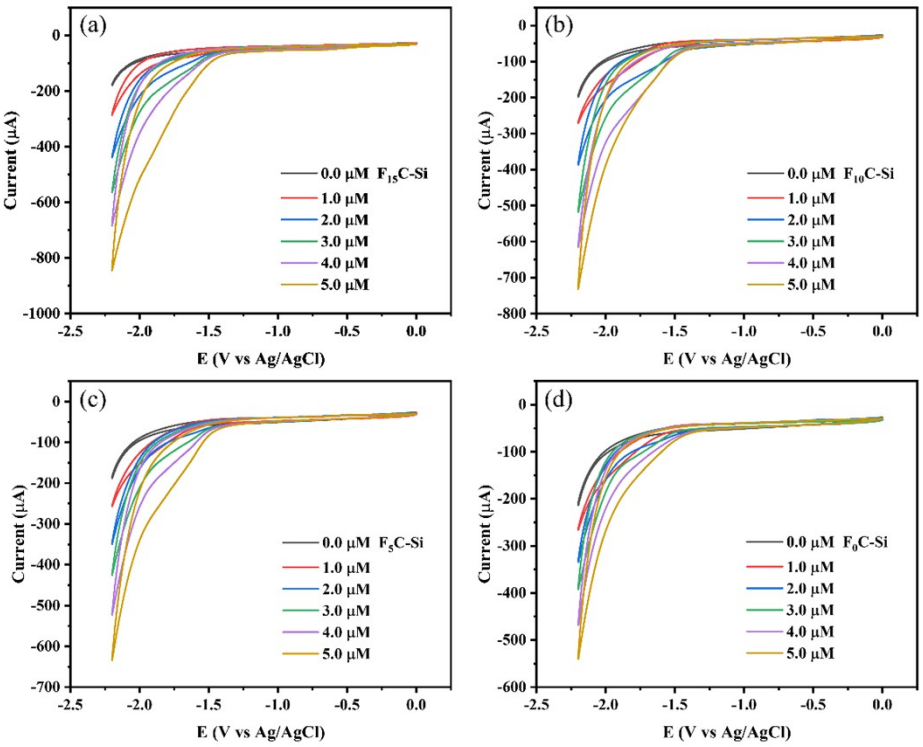

Fig. S38 CVs of various concentrations of F_{15}C-Si, F_{10}C-Si, F_5C-Si and F_0C-Si (0.0 μM–5.0 μM) in buffer solutions at pH=7.0 (V_{MeCN}/V_{H2O} = 2/3).

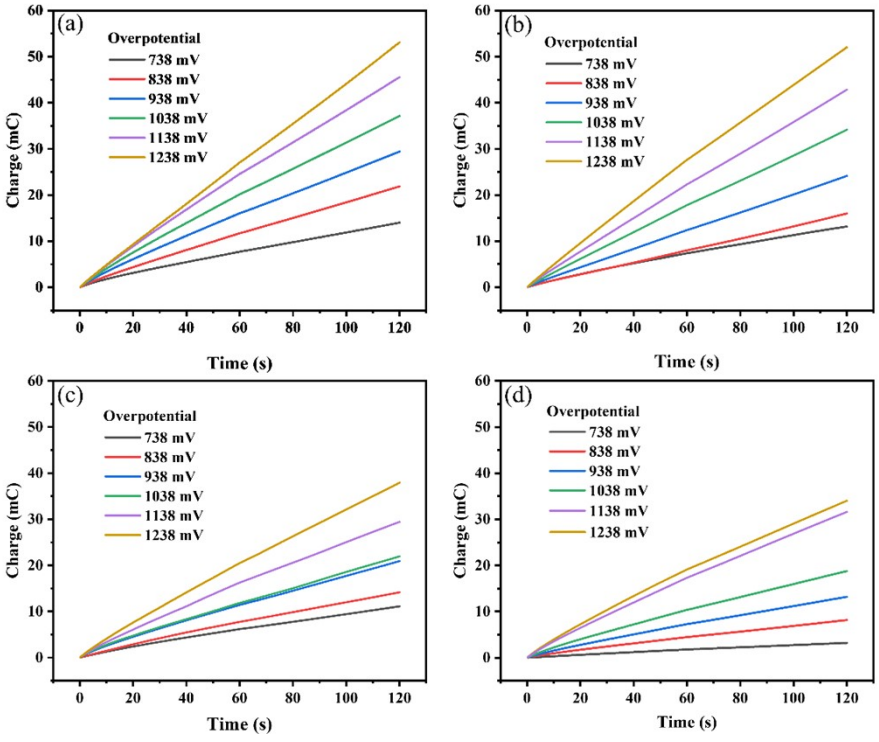

Fig. S39 Charge accumulation of electrolyzing 5 μM F_{15}C-Si, F_{10}C-Si, F_5C-Si and F_0C-Si at a range of overpotentials in buffer solutions at pH=7.0 for 2 minutes (a-d).

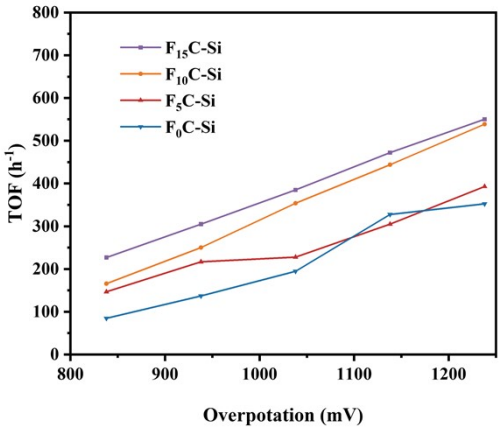

Fig. S40 TOF values of 5 μM F_{15}C-Si, F_{10}C-Si, F_5C-Si and F_0C-Si at different overpotentials in buffer solutions at pH=7.0.

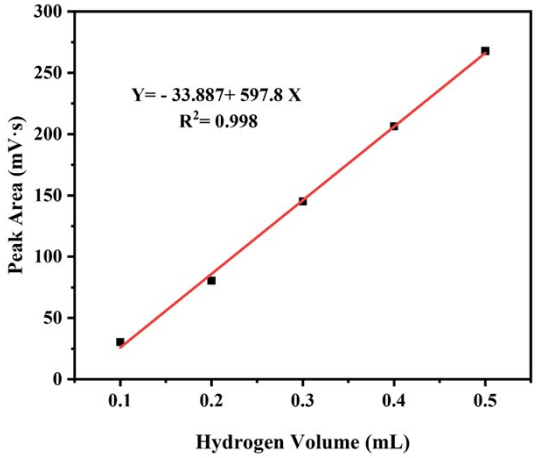

Fig. S41 The hydrogen calibration plot from GC measurements.

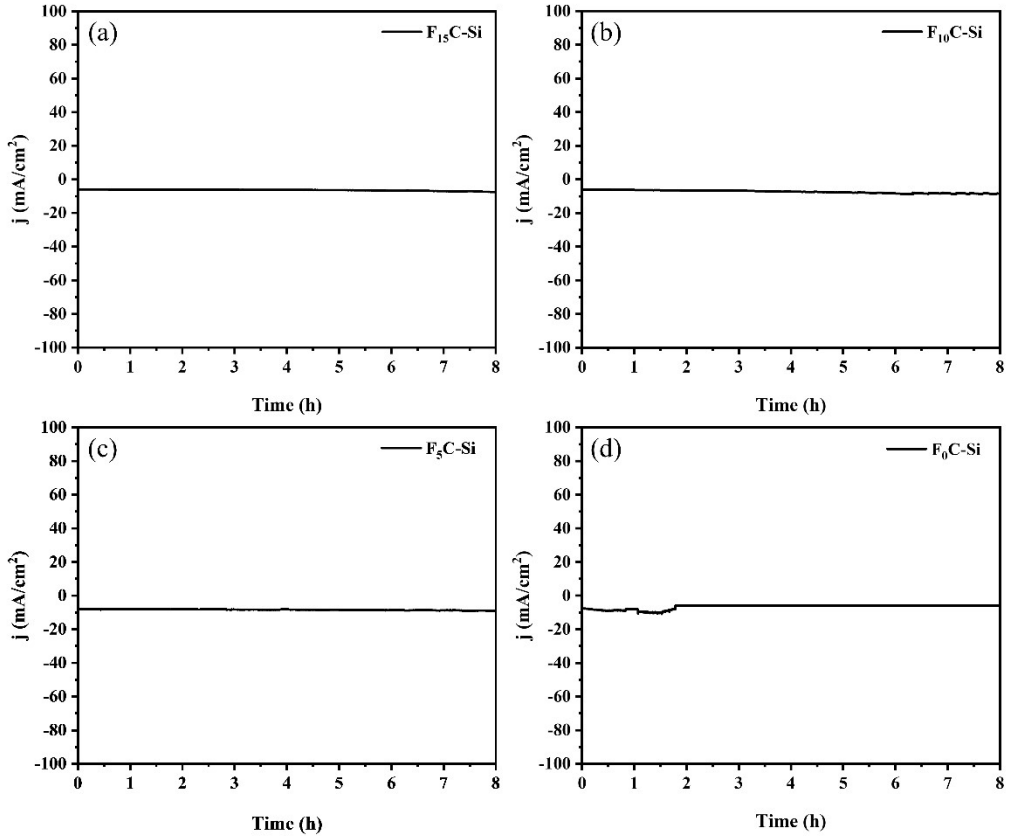

Fig. S42 Current versus 5 μM F_{15}C-Si, F_{10}C-Si, F_5C-Si and F_0C-Si in buffer solution at pH = 7.0 at -2.2 V for 8 h electrolysis.

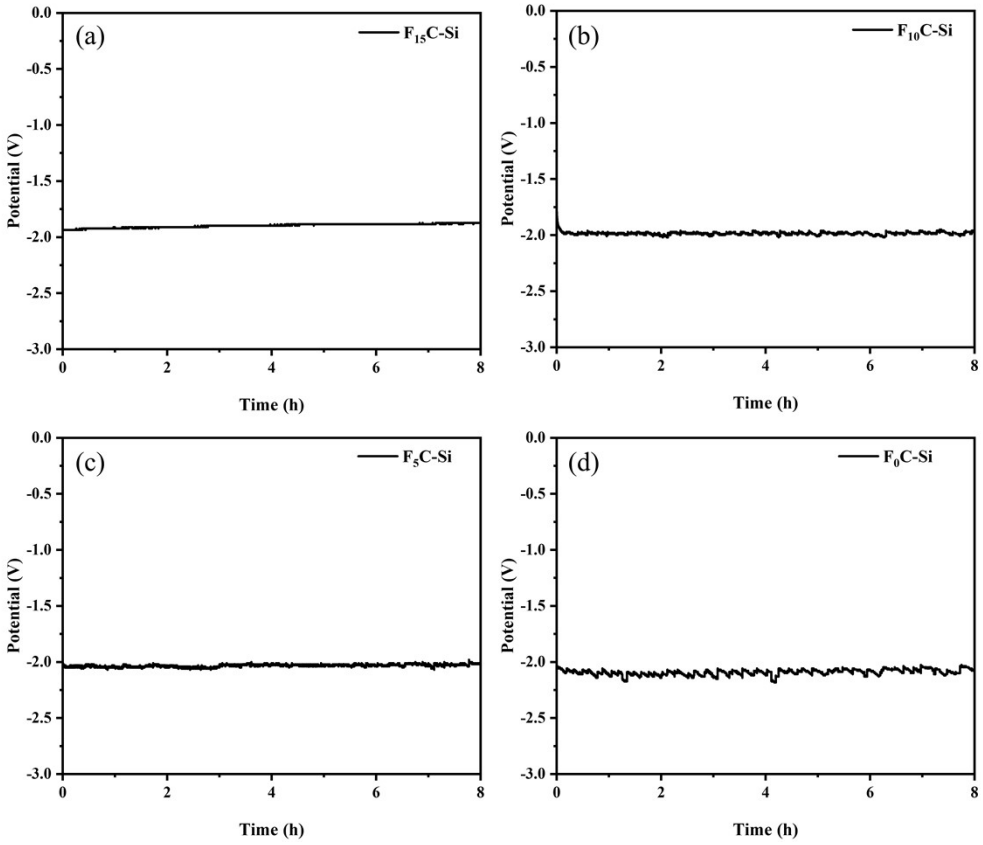

Fig. S43 Voltage variation versus 5 μM F_{15}C-Si, F_{10}C-Si, F_5C-Si, and F_0C-Si in buffer solution at pH = 7.0 under constant current electrolysis at 400 μA for 8 h.

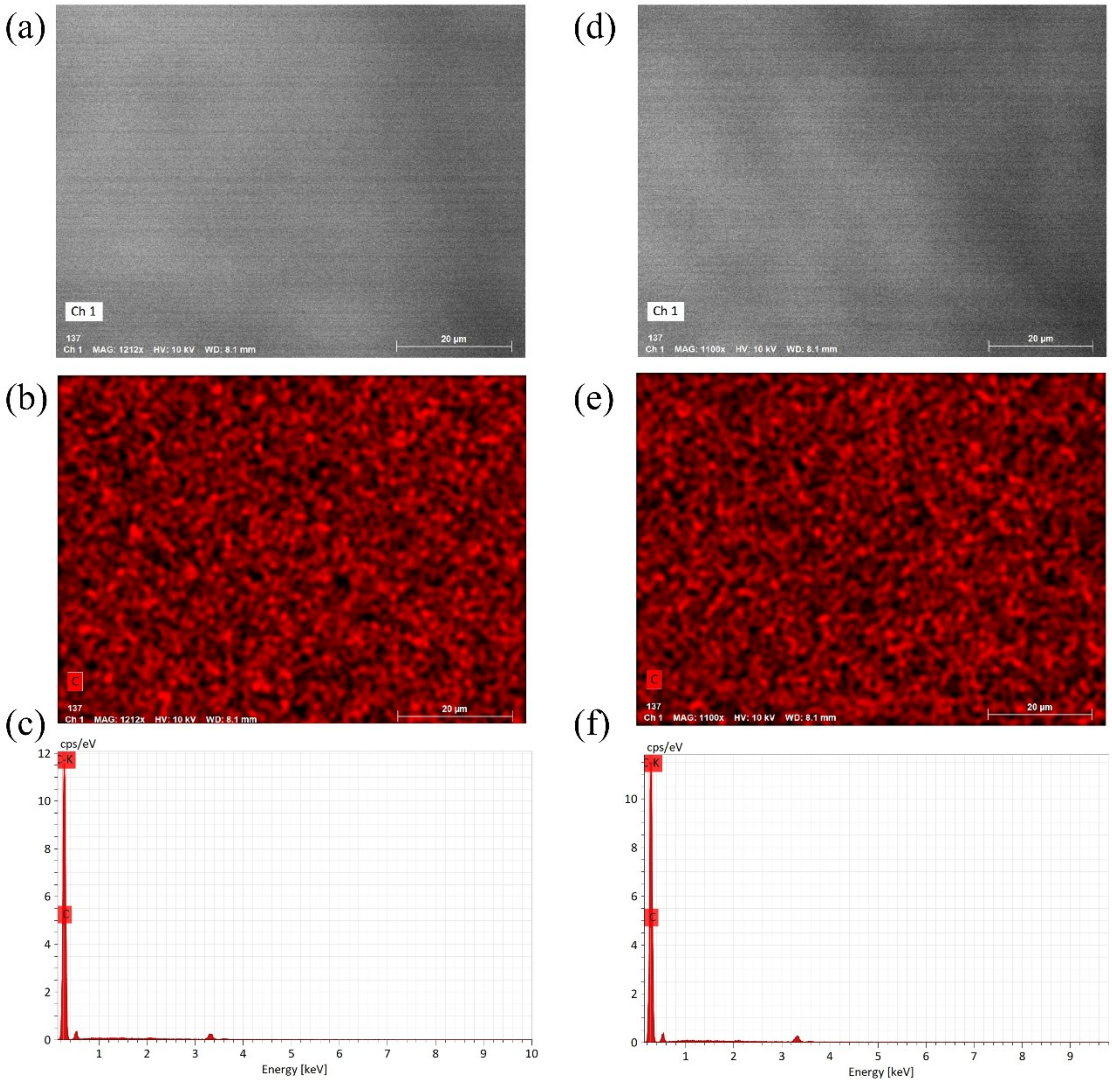

Fig. S44 SEM images and EDX data of GC electrodes before (a-c) and after (d-f) electrolysis.

Table S1 Performance parameters of four corroles F_{15}C-Si, F_{10}C-Si, F_5C-Si and F_0C-Si in DMF containing 16 mM TFA

complex	i_{cat}/i_p	Overpotential, mV	TOFmax, s^{-1}	C.E
F_{15}C-Si	12.38	973	173.19	0.39
F_{10}C-Si	11.77	1004	125.56	0.37
F_5C-Si	9.50	1047	97.62	0.30
F_0C-Si	7.07	1061	85.41	0.22

Table S2 Performance parameters of four corroles F_{15}C-Si, F_{10}C-Si, F_5C-Si and F_0C-Si in DMF containing 16 mM TsOH

complex	i_{cat}/i_p	Overpotential, mV	TOFmax, s^{-1}	C.E
F_{15}C-Si	31.08	1135	752.65	0.97
F_{10}C-Si	25.43	1141	614.02	0.79
F_5C-Si	21.14	1199	531.67	0.66
F_0C-Si	20.55	1216	397.28	0.64

Table S3 The turnover frequency (TOF) of silicon corroles and transition metal complexes in aqueous phase.

complex	TOF(h^{-1})	Overpotential, mV	Solution	Reference
$F_{15}C$-Si	550.26	1238	Buffer	This work
$F_{10}C$-Si	538.86	1238	Buffer	This work
F_5C-Si	392.95	1238	Buffer	This work
F_0C-Si	327.56	1238	Buffer	This work
BPTC-Co	567	1088	Buffer	[5]
PFIC-Co	405	1038	Buffer	[6]
Fe(TPFC)Cl	274	838	Water	[7]
BPXSC-Co	517	1138	Buffer	[8]
BPXHC-Co	526	1138	Buffer	[8]
Cu(HL)Cl	482	837	Buffer	[9]
CoOHC	1447.4	988	Buffer	[10]
Co-BPNC-PPh_3	450	838	Buffer	[11]
$(ClO_4)_2$	230	900	Buffer	[12]

References:

(1) S. Mondal, A. Garai, P. K. Naik, J. K. Adha and S. Kar, *Inorg Chim Acta*, 2020, **501**, 119300.

(2) L. Huang, A. Ali, H. Wang, F. Cheng and H. Liu, *Journal of Molecular Catalysis A: Chemical*, 2017, **426**, 213-222.

(3) I. Luobeznova, M. Raizman, I. Goldberg and Z. Gross, *Inorg Chem*, 2006, **45**, 386-394.

(4) K. Ueta, M. Fukuda, G. Kim, S. Shimizu, T. Tanaka, D. Kim, A. Osuka, *Chem. -A Eur. J.* 2018, **24(30)**, 7637-7646.

(5) J.-X. Hao, Z.-W. Liu, S.-Y. Xu, L.-P. Si, L.-M. Wang , H.-Y. Liu, *Inorganica Chimica Acta*. (2024), **564**, 121967.

(6) L.-W. Wu, Y.-F. Yao, S.-Y. Xu, X.-Y. Cao, Y.-W. Ren, L.-P. Si , H.-Y. Liu, *Catalysts*. (2024), **14(1)**: 5.

(7) Y.-Q. Zhong, M. S. Hossain, Y. Chen, Q.-H. Fan, S.-Z. Zhan , H.-Y. Liu, *Transition Metal Chemistry*. (2019), **44**, 399-406.

(8) X.-Y. Cao, S.-Y. Xu, L.-W. Wu, Y.-F. Qiu, H. Zhang, L.-P. Si, L.-M. Wang , H.-Y. Liu, *Catalysis Science & Technology*. (2024), **14**, 5608-5615.

(9) R.-Z. Liao, M. Wang, L. Sun , P. E. M. Siegbahn, *Dalton Transactions*. (2015), **44**, 9736-9739.

(10) Z.-Y. Lv, G. Yang, B.-P. Ren, Z.-Y. Liu, H. Zhang, L.-P. Si, H.-Y. Liu , C.-K. Chang, *European Journal of Inorganic Chemistry*. (2023), **26,** e202200755.

(11) H. Chen, D.-L. Huang, M. S. Hossain, G.-T. Luo , H.-Y. Liu, *Journal of Coordination Chemistry*. (2019), **72**, 2791-2803.

(12) L. van Dijk, M. J. Tilby, R. Szpera, O. A. Smith, H. A. P. Bunce , S. P. Fletcher, *Nature Reviews Chemistry*. (2018), **2**, 0117.